

Incremental Learning of Sparse Attention Patterns in Transformers

Oğuz Kaan Yüksel*
TML Lab, EPFL

oguz.yuksel@epfl.ch

Rodrigo Alvarez Lucendo
TML Lab, EPFL

rodrigo.alvarezlucendo@epfl.ch

Nicolas Flammarion
TML Lab, EPFL

nicolas.flammarion@epfl.ch

Abstract

This paper introduces a high-order Markov chain task to investigate how transformers learn to integrate information from multiple past positions with varying statistical significance. We demonstrate that transformers learn this task incrementally: each stage is defined by the acquisition of specific information through sparse attention patterns. Notably, we identify a shift in learning dynamics from competitive, where heads converge on the most statistically dominant pattern, to cooperative, where heads specialize in distinct patterns. We model these dynamics using simplified differential equations that characterize the trajectory and prove stage-wise convergence results. Our analysis reveals that transformers ascend a complexity ladder by passing through simpler, misspecified hypothesis classes before reaching the full model class. We further show that early stopping acts as an implicit regularizer, biasing the model toward these simpler classes. These results provide a theoretical foundation for the emergence of staged learning and complex behaviors in transformers, offering insights into generalization for natural language processing and algorithmic reasoning.

1 Introduction

Knowledge is often compositional and hierarchical in nature. As such, understanding complex concepts often requires an *incremental* approach, where simpler concepts are learned first and then combined to form more complex ideas. Such incremental approaches are crucial for various cognitive tasks, including language comprehension, problem-solving, and decision-making in humans and has been recapitulated in machine learning in various settings (Saxe et al., 2019). In particular, language, is inherently hierarchical, e.g., understanding a sentence requires understanding the meanings of individual words, phrases, and their structure. Consequentially, there has been interest in understanding *incremental* learning behavior of transformers in sequential tasks (Abbe et al., 2023b; Edelman et al., 2024), particularly in how they build upon previously learned information to understand and generate language (Chen et al., 2024a).

The elementary operation that is needed to compose information is *copying*, which is used to duplicate data and then perform downstream computations. In language, copying is essential for tasks such as text generation, where the model must replicate certain phrases or structures from the input to produce coherent and contextually relevant output (Olsson et al., 2022), and, as a means to aggregate information from multiple parts of a text to form a comprehensive understanding. Copying is also a fundamental operation in algorithmic reasoning, where it is often necessary to duplicate intermediate results to perform further computations. Transformers implement this operation across different positions via sparse attention patterns which pushes their parameters to diverge. Therefore, the dynamics of how these circuits are established

*Corresponding author.

and its implications on reasoning, generalization and emergence are crucial to grasp the inner workings of transformers.

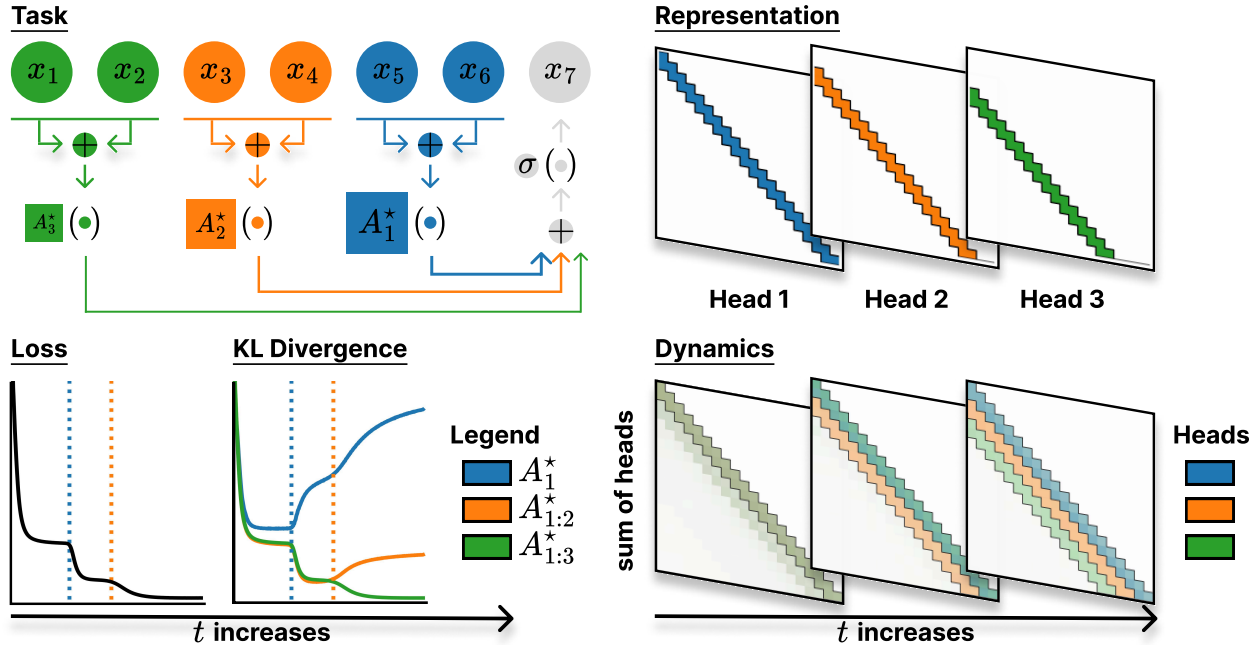


Figure 1: (Top left) The task is based on a high-order Markov chain, where the next token depends on multiple past tokens with different importance weights. The context is divided into different groups of positions, each aggregated and processed by an associated feature matrix A_k^* of various importance which is represented by the size of the feature matrix. (Top right) An idealized representation of the task in a multi-head single-layer attention. Each head represents an individual sparse attention pattern required to solve the task. (Bottom left) Transformers learn the task incrementally, with each stage corresponding to the acquisition of a sparse attention pattern which is indicated by the KL divergence between predictors $A_{1:i}^*$ that only depends a subset of relevant positions as defined in Equation (3) and the transformer. (Bottom right) The learning dynamics transition from competitive, where all heads focus on the statistically most important pattern (indicated by high combined attention on the main diagonal), to cooperative, where different heads specialize in different patterns.

In this paper, we study single-block decoder-based transformers and the formation of sparse attention circuits during training. Simplest such circuit is the “copying” circuit that focused on exactly one position. It is a subcircuit of well-known *induction heads* in transformers (Elhage et al., 2021; Olsson et al., 2022). Sparse attention circuits are the building blocks that allow models to duplicate information from one part of the input to another, enabling the integration of information across multiple positions. We show that they are learned incrementally, with the model first acquiring the ability to copy from the most statistically important pattern, as they provide the most significant improvement in prediction accuracy, and then progressively learning the less important patterns. Interestingly, we observe an initial dynamics where all heads compete to learn the most important pattern, followed by a transition to a cooperative phase where different heads specialize in different patterns. We explain these dynamics using a set of simplified differential equations, after simplifications to the architecture and the task. This leads to connections to tensor factorization which is a well-studied problem (Arora et al., 2019; Razin et al., 2021; Li et al., 2021; Jin et al., 2023).

Our main contributions are as follows:

- We establish the simplest setting for positional incremental learning in transformers. In particular, we isolate the importance of sparse attention patterns as the driving force for incremental learning

in transformers, requiring only a single self-attention layer compared to more intricate in-context learning settings such as (Edelman et al., 2024).

- We show that the learning dynamics transition from competitive, where all heads focus on the statistically most important positions, to cooperative, where different heads specialize in different positions. We provide a convergence result characterizing the initial competitive phase as a system of coupled dynamics driven by symmetric initialization. Building on this, we establish convergence for the cooperative phase by analyzing the trajectories initialized in the vicinity of intermediate saddle points.
- We run studies to understand the impact of the incremental training dynamics on generalization. Depending on the size of the training set, models have different attention patterns, e.g., with a smaller training set, the model learns to copy only from the most important positions. This suggests that there is a regularization induced by the training trajectories, where transformers are pushed to be misspecified depending on the size of the training set. With early stopping, this may result in sample complexity benefits in low-data regimes.

2 Stage-wise Formation of Sparse Attention Patterns

In this section, we describe the data generation process, how transformers can solve it and the experimental evidence towards incremental learning of sparse attention patterns in transformers.

2.1 Markov Chains with Importance Structure

We consider a sequential classification task based on a discrete Markov chain of order w with states $\mathcal{D} = \{1, \dots, d\}$. To facilitate the transition dynamics in a vector space, we represent each state i by its one-hot encoding $e_i \in \mathbb{R}^d$. Consequently, each element x_t in the generated sequence is a one-hot vector.

The sequence is initialized by sampling the first w tokens independently and uniformly:

$$x_{-w+1}, \dots, x_0 \stackrel{\text{i.i.d.}}{\sim} \text{Unif}(\mathcal{D}) .$$

For $t \in [0, T - 1]$, the next state x_{t+1} is sampled from a categorical distribution whose parameters are determined by a weighted combination of past states:

$$x_{t+1} \sim \text{Categorical} \left(\text{softmax} \left(\sum_{k=1}^h A_k^* \sum_{i \in I(k)} \alpha_i x_{t-i} \right) \right), \quad (1)$$

where $A_k^* \in \mathbb{R}^{d \times d}$ are fixed feature matrices, $I(k)$ are disjoint sets that partition $\{0, \dots, w - 1\}$ and α_i are importance weights which satisfy $\sum_{i \in I(k)} \alpha_i = 1$ for all $k \in [h]$. This task is simple yet non-trivial and captures some features relevant to practice: (i) it is sequential, requiring the model to integrate information from past positions, (ii) it has a positional structure, as each component of the prediction depends on a subset of the past states, and (iii) different positions can have different importance, as determined by the feature matrices A_k^* and scalars α_i .

As $I(k)$ and A_k^* can be permuted without changing the data generation process, we assume without loss of generality that $\|A_1^*\| \geq \|A_2^*\| \geq \dots \geq \|A_h^*\|$ and that $I(1)$ contains the most important positions, i.e., those associated with the largest feature norms. In general, there can be different spectrums of importance within each feature matrix as well as within each $I(k)$ via α_i .

One particular choice of interest is to have $I(k)$ to be contiguous blocks of indices that start from the most recent position, i.e., for some $0 = i_0 < i_1 < i_2 < \dots < i_{h-1} < i_h = w - 1$,

$$I(i) = \{i_0, \dots, i_1\}. \quad (2)$$

This choice is inspired by the natural language where nearby tokens that complete the text into a word or a short phrase should have more statistical correlation over the distant tokens. Notably, when each of

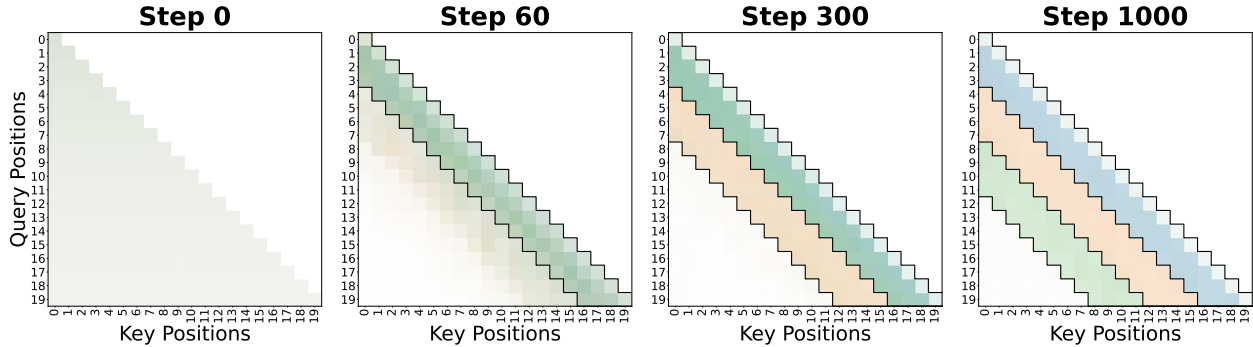


Figure 2: The sum of learned attention patterns for $h = 3, w = 12$ at different stages of training where blue, yellow and green colors correspond to different heads. At $t = 0$, the attention is uniform as the model is randomly initialized. At $t = 60$, all heads learn from the positions in $I(1)$, indicated by the overlapping blue, yellow and green colors, with one head focusing on the positions in $I(2)$ with a small attention. At $t = 300$, a head learns from the positions in $I(2)$ whereas two heads still focus on $I(1)$. At $t = 1000$, the model finally learns to integrate all positions where each head specializes in a different pattern. The main diagonal does not have the same intensity as the other positions as it is learned via the skip connection directly from the input.

the $I(k)$ are singletons, the resulting operation is copying from a particular position and then processing it with a linear feature map. The “copying” operation is of particular interest as it appears in various settings including in-context learning (Brown et al., 2020).

2.2 Transformers Learn Incrementally

We train single-block decoder-based transformers with h heads on sequences sampled as in Equation (1) by minimizing the cross entropy loss over the full sequence except the initial tokens x_{-w+1}, \dots, x_0 that are not sampled from the process. We keep the architecture as close to the standard practice as possible. The architecture and optimization details are provided in Appendix A.

We sample feature matrices A_k^* uniformly over orthogonal matrices and then scale with positive scalars m_k . These constants are chosen geometrically, i.e., $m_k = m^{h-k}b_0$ where $m > 1$ is the multiplicative constant and $b_0 > 0$ is the base scale. This results in an importance hierarchy in the feature matrices whereas features within the same matrix has the same importance. In particular, A_1^* has the largest norm and thus contains the most influential features in the process whereas A_h^* has the smallest norm and thus the least important features. For simplicity, we choose $\alpha_i = 1/|I(I^{-1}(i))|$ where I^{-1} is the inverse of I . Lastly, we choose $I(k)$ as in Equation (2) with the same length intervals of size w/h . These choices formalize the notion of relative importance between local positions over the distant positions. As $I(1)$ is paired with A_1^* that has a large norm, the nearby positions influence the next token more than the distant tokens in $I(h)$ that are paired with A_h^* which has a small norm. The details of all experimental parameters are provided in Appendix A and additional experiments can be found in Appendix B.

We observe that the transformers learn the task incrementally, with each stage corresponding to the acquisition of a sparse attention pattern as in Figure 2. All heads start at uniform due to the initialization. Then, they first mainly focus on the positions in $I(1)$ as they are the most statistically important positions. At this stage, the heads compete to learn from these positions, resulting in overlapping attention patterns with some deviations due to the initialization. Later, heads gradually specialize in different patterns, with one head learning from the positions in $I(2)$ while the other finally focusing on $I(3)$.

In order to understand the dynamics in the function space, we train models with different maximum context lengths $c = 4, 8, 12$. When $c = 4$, the model can only access the positions in $I(1)$ and thus learns only from these positions. When $c = 8$, the model can access the positions in $I(1)$ and $I(2)$ and when $c = 12$, the model can access all the relevant positions and can implement the task perfectly. In Figure 3 (right), we plot the Kullback-Leibler (KL) divergence between the predictions of these transformers and the transformer without

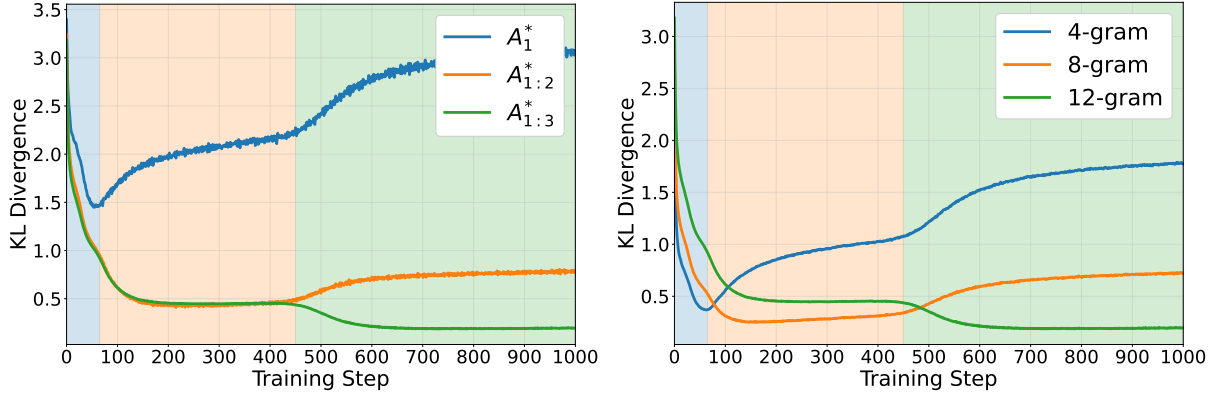


Figure 3: (Left) KL divergence between the ground truths that only depend on the positions in $I(1)$, $I(1) \cup I(2)$ and $I(1) \cup I(2) \cup I(3)$, and the predictions of the transformer with unrestricted context length. (Right) KL divergence between the predictions of the transformers with restricted context lengths $c = 4, 8, 12$ and the transformer without any context length restriction. The transformers learn the task incrementally, with each stage corresponding to the acquisition of information from a subset of positions.

any context length restriction. We observe that the transformers first approach the model with $c = 4$ and then $c = 8$ before finally reaching the full model with $c = 12$. This indicates that the transformers not only learn the attention patterns but also simultaneously learn the feature matrices associated with these patterns.

Similarly, we study the KL divergence pattern when comparing the predictions of the transformers to the ground truths that only depend on the positions in $I(1)$, $I(1) \cup I(2)$ and $I(1) \cup I(2) \cup I(3)$:

$$f_{A_{1:i}^*} = \text{softmax} \left(\sum_{k=1}^i A_k^* \sum_{j \in I(k)} \alpha_j x_{t-j} \right). \quad (3)$$

This is plotted in Figure 3 (left) where we see an identical pattern. These are similar to what Edelman et al. (2024) observed for in-context Markov chain where stages are characterized by sub- n -grams.

2.3 Representation with a Simplified Multi-Head Attention

Here, we construct a simple representation on a single-layer multi-head attention that solves the task. Let $X \in \mathbb{R}^{d \times (T+w)}$ be the input data matrix with columns $x_{-w+1}, \dots, x_0, x_1, \dots, x_T$. We assume that the positional information is encoded using one-hot vectors in \mathbb{R}^T and concatenated to the data as follows:

$$\tilde{X} = \begin{pmatrix} X \\ I_{T+w} \end{pmatrix} \in \mathbb{R}^{(d+T+w) \times (T+w)}.$$

We denote the columns of \tilde{X} as $\tilde{x}_i \in \mathbb{R}^{d+T+w}$, representing the position-augmented embedding of the i -th token. Then, the transformer takes \tilde{X} as input and produces the output $Y \in \mathbb{R}^{d \times T}$ with columns y_0, \dots, y_{T-1} as follows:

$$y_t = \text{softmax} \left(\sum_{k=1}^h V_k \tilde{X} a_t^{(k)} \right), \quad \text{with} \quad a_t^{(k)} = \text{softmax} \left(\mathcal{M}_{T-t} \left(\tilde{X}^\top K_k^\top Q_k \tilde{x}_t \right) \right),$$

where $Q_k, K_k, V_k \in \mathbb{R}^{(d+T+w) \times (d+T+w)}$ are the query, key and value matrices of the head k , respectively and \mathcal{M}_p sets the last p entries to $-\infty$ to apply causal masking.

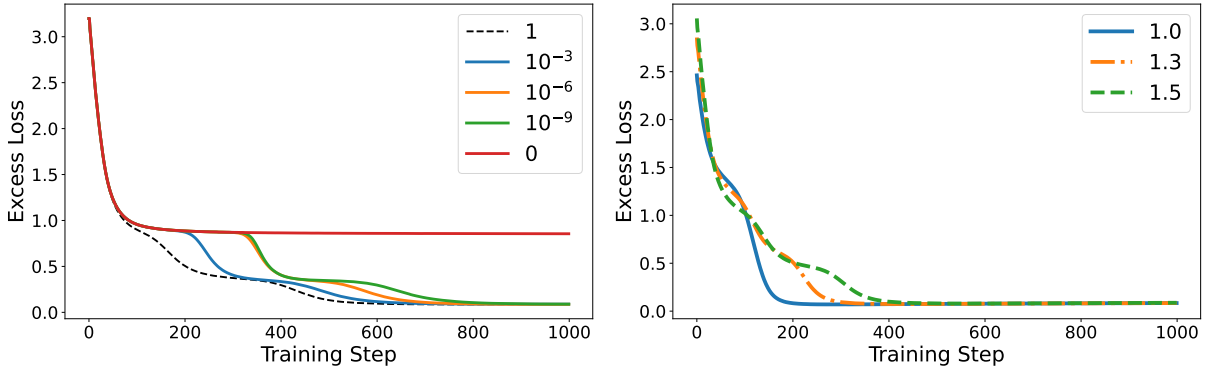


Figure 4: (Left) Excess loss of the minimal architecture with different initialization scales. (Right) Excess loss of the minimal architecture with different multiplicative constants m that determine the importance hierarchy.

For head k , we set the value matrix $V_k = A_k^*$ and $a_t^{(k)}$ to be a positional-only attention corresponding to $I(k)$ with the following sparse pattern

$$\frac{1}{|I(k)|} \left(\underbrace{0, \dots, 0}_t, \underbrace{\mathbf{1}_{(w-1) \in I(k)}, \mathbf{1}_{(w-2) \in I(k)}, \dots, \mathbf{1}_{0 \in I(k)}}_w, \underbrace{0, \dots, 0}_{(T-t)} \right).$$

Here, the first t entries correspond to the irrelevant tokens in the context and the last $(T - t)$ entries are zeroed out due to the causal masking. Among the relevant tokens in the intermediate w positions, the attention focuses on the indices in $I(k)$ as they can be processed altogether with the same feature matrix $V_k = A_k^*$. As the target patterns are sparse, the parameters of the attention need to diverge to infinity to exactly learn this operation. In practice, we expect finite values that approximate these sparse attention patterns. These attention patterns can be learned based on the positional information:

$$K_k^\top Q_k = \lambda \sum_{i \in I(k)} \sum_{p=w}^{T+w} e_{d+p-i} e_{d+p}^\top,$$

where $\lambda > 0$ is a scaling constant and e_i is the i -th standard basis vector in \mathbb{R}^{d+T} . As $\lambda \rightarrow \infty$, the attention scores converge to the desired sparse pattern.

Note that this construction is not unique as there are many Q_k and K_k that can realize the same attention pattern. In particular, there is a symmetry where (Q_k, K_k) can be replaced with $(M^{-1}Q_k, M^\top K_k)$ for any invertible matrix M without changing the attention scores. Moreover, as there are h heads to learn, the construction has a permutation symmetry. The permutation symmetry is key in understanding the learning dynamics, as we discuss in Section 3.2.

2.4 Ablation Studies

In order to isolate the essential components that drive the incremental learning behavior, we simplify the architecture by removing some components. First, we remove any components such as layer normalization and residual connections that are not present in the idealized construction in Section 2.3. Then, we reduce the product $K_k^\top Q_k$ to a single matrix A_k as there is a symmetry between K_k and Q_k . All of these changes individually or combined do not alter the incremental learning behavior. We plot the learning behavior of this simplified model in Figure 1.

We also perform ablation studies with this minimal architecture. We first vary the initialization scale of the attention matrices A_k and set value matrices to be zero. While initializing A_k , we use uniform distribution

over $[-u, u]$ where u is the initialization scale. Figure 4 (left) shows that the speed of incremental learning is affected by the initialization scale, with smaller scales resulting in slower learning. At the extreme $u = 0$, we observe that the model only learns a single pattern and does not progress further. This is because of the symmetry between the heads, which requires a small perturbation to break.

We also vary the multiplicative constant m that determines the structure in the data generation process. Figure 4 (right) shows that the number of steps diminish to two for $m = 1$, where there is no importance ordering. Qualitatively, this model first learns a single pattern and then the other two are learned simultaneously. For $m = 1.3$ and $m = 1.5$, we still observe three distinct stages, but the stages are intertwined for $m = 1.3$ and bumps are less pronounced.

2.5 Dataset Size and Generalization

Lastly, we study the effect of the dataset size on the incremental learning behavior. As we decrease the dataset size and cross some critical thresholds, we observe that the number of stages that occur in training decreases, as seen in Figure 5 (left). Figure 5 (right) plots the KL divergence between the predictions of the model with different context lengths and the trained transformer. The trend is similar to the one observed in Figure 3 but with different number of bumps for each dataset size.

This points towards a beneficial regularization from the training trajectory which leads to misspecified models, i.e., models that are not able to learn the task perfectly as they have a shorter context length. Yüksel et al. (2025) argue that such misspecification can be beneficial in low-data regimes, making learning statistically feasible. Notably, transformers with early stopping seem to select the misspecification length automatically, hinting at potential sample complexity gains in these settings.

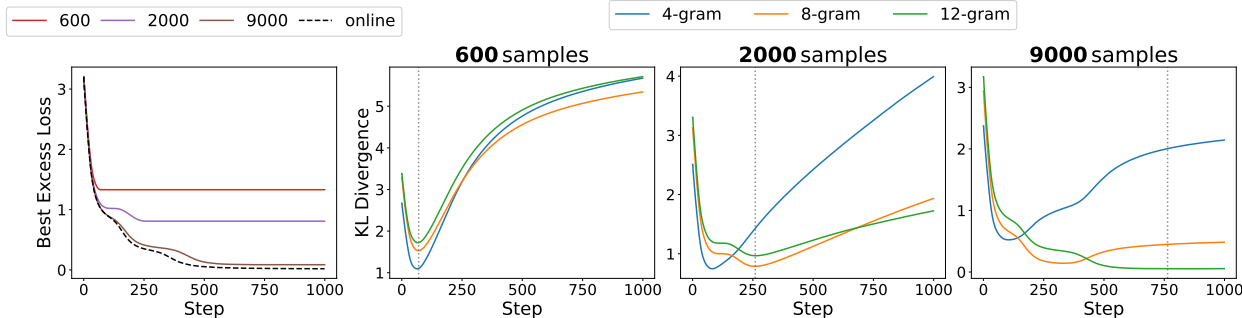


Figure 5: The impact of the dataset size on the incremental learning behavior. (Left) The best validation loss as a function of the dataset size. (Right) The KL divergence between the predictions of the model with different context lengths and the trained transformer. Dashed lines indicate the first step that obtains the best excess loss.

3 Training Dynamics on Regression Variant

In this section, we study the regression variant of the classification task in Section 2.1. We study the resulting training dynamics by analyzing the gradient flow dynamics of the loss.

3.1 The Regression Model

Consider the following regression task associated to any distribution \mathcal{P}_X and \mathcal{P}_ξ :

$$(x_1, \dots, x_T) \sim \mathcal{P}_X, \xi \sim \mathcal{P}_\xi, \quad \text{and} \quad y^*(X) = \sum_{k=1}^h A_k^* X s_k^* + \xi,$$

where $s_k^* \in \mathbb{R}^T$ is the vector with entries α_i for $i \in I(k)$ and zero otherwise. For this section, we set $|I(k)| = 1$ for all k for simplicity. Let $m_k^* = \|A_k^*\|_F$, $V_k^* = \frac{A_k^*}{m_k^*}$ for all $k \in [h]$ with $m_1^* > \dots > m_h^*$ without loss of generality.

We make some assumptions regarding the distributions $\mathcal{P}_X, \mathcal{P}_\xi$ and the feature matrices.

Assumption 1. *The noise is zero-mean, i.e., $\mathbb{E}[\xi] = 0$ and the data is normalized, i.e.,*

$$\forall i, j \in [T], \quad \mathbb{E}[x_i x_j^\top] = \mathbf{1}_{i=j} I_d.$$

Assumption 2. *The feature matrices are orthogonal, i.e.,*

$$\forall i, j \in [h], \quad \langle V_i^*, V_j^* \rangle = \text{Tr}((V_i^*)^\top V_j^*) = \mathbf{1}_{i=j}.$$

We use the minimal architecture obtained in Section 2.4 with the following modifications. The attention scores are computed only via the inner product of position vectors instead of the concatenated position and data vectors. As the problem is a regression task on the final token, we only need the last row of the matrix Q_k which we denote by $q_k \in \mathbb{R}^T$. Then, the resulting model is as follows:

$$y_\theta(X) = \sum_{k=1}^h V_k X s_k, \quad \text{with } s_k = \text{softmax}(q_k),$$

where $\theta = (V_1, \dots, V_h, q_1, \dots, q_h)$ are the learnable parameters. We set the loss to the mean square loss:

$$\mathcal{L}(\theta) = \frac{1}{2} \mathbb{E}_{x_1, \dots, x_T, \xi} [\|y_\theta(X) - y^*(X, \xi)\|^2]. \quad (4)$$

We study the gradient flow dynamics of the population loss in Equation (4), i.e., we consider the continuous-time limit of gradient descent with infinitesimal step size.

Tensor Notation. We construct tensors that are sum of outer products of matrices and vectors, i.e., $\mathbf{M} = \sum_{k=1}^h B_k \otimes v_k$ where $B_k \in \mathbb{R}^{d \times d}$ and $v_k \in \mathbb{R}^T$. The product $X^\top \mathbf{M}$ denotes $X^\top \mathbf{M} = \sum_{k=1}^h \langle B_k, X \rangle v_k$ whereas the product $\mathbf{M}v$ denotes $\mathbf{M}v = \sum_{k=1}^h B_k \langle v_k, v \rangle$. The inner product between two tensors $\mathbf{M} = \sum_{k=1}^h B_k \otimes v_k$ and $\mathbf{N} = \sum_{k=1}^h B'_k \otimes v'_k$ is denoted by $\langle \mathbf{M}, \mathbf{N} \rangle = \sum_{k=1}^h \langle B_k, B'_k \rangle \langle v_k, v'_k \rangle$. The Frobenius norm of a tensor \mathbf{M} is given by $\|\mathbf{M}\|_F = \sqrt{\langle \mathbf{M}, \mathbf{M} \rangle}$.

Proposition 1 reinterprets this dynamics as a gradient flow of a tensor factorization problem.

Proposition 1. *The gradient flow dynamics of the loss in Equation (4) is equivalent to that on*

$$\mathcal{L}(\theta) = \frac{1}{2} \|\mathbf{G} - \mathbf{P}\|_F^2 \quad \text{where } \mathbf{P} = \sum_{k=1}^h V_k \otimes s_k, \quad \text{and } \mathbf{G} = \sum_{k=1}^h m_k^* (V_k^* \otimes s_k^*).$$

Attention Reparameterization. Note that due to the softmax operation, $\sum_i q_i$ is always constant and thus we can restrict q_k to have a zero mean without loss of generality. This implies that, there is a one-to-one correspondence between q_k and s_k in the subspace of zero-mean vectors. Therefore, it is possible to analyze the dynamics in terms of s_k instead of q_k with the notation $\Pi(s) = (\text{diag}(s) - ss^\top)$:

$$\dot{V}_k = (\mathbf{G} - \mathbf{P}) s_k, \quad \dot{s}_k = \Pi(s_k)^2 (V_k^\top (\mathbf{G} - \mathbf{P})).$$

Numerical Simulations. We simulate these differential equations with initialization $V_i = 0$ and $s_i \approx \frac{1}{T} \mathbf{1}_T$. The results recapitulate the incremental learning behavior observed in Figure 2. We present the results in Section B.4.

3.2 Coupled Dynamics Describe the Competitive Phase

We show that the competitive phase of the learning dynamics can be described by the symmetric initialization $s_1(0) = s_k(0), V_1(0) = V_k(0)$ for all k . Once the heads are coupled, they coevolve, i.e., $s_k(0) = s(0), V_k(0) = V(0)$ for all k .

This leads to the following coupled dynamics:

$$\dot{V} = (\mathbf{G}s - h\|s\|^2V), \quad \dot{s} = \Pi(s)^2 (V^\top \mathbf{G} - h\|V\|_F^2 s).$$

Theorem 1. *Assume that the initialization verifies the following for all $k \in [h]$:*

$$\langle V(0), V_1^* \rangle \geq \langle V(0), V_k^* \rangle, \quad \langle s(0), s_1^* \rangle \geq \langle s(0), s_k^* \rangle. \quad (5)$$

Then, the dynamics of V and s converge to the following fixed point:

$$V(\infty) = \frac{m_1^*}{h} V_1^*, \quad s(\infty) = s_1^*. \quad (6)$$

Theorem 1 is based on an ordering argument. As long as the initialization verifies the ordering condition in Equation (5), the dynamics of V and s are such that \dot{V} and \dot{s} reinforces the same order. Standalone, Theorem 1 does not explain what happens when the heads do not start with the same initialization. Theorem 2 establishes that when many heads are initialized with a small deviation from the symmetric initialization, the deviation from the symmetric initialization is bounded for a finite time that we can precisely control. Therefore, the initialization chooses the coupling time of different heads after which they might start to diverge.

Theorem 2. *Assume that the following holds for $\epsilon \ll 1$:*

$$\forall k \in [h] : \|V(0) - V_k(0)\|_F \leq \epsilon \text{ and } \|s(0) - s_k(0)\|_2 \leq \epsilon.$$

Then, there exists a constant c_1 such that $\forall t \in \left[0, \frac{1}{-c_1 \log \epsilon}\right]$:

$$\|V_k(t) - V(t)\|_F \leq \epsilon e^{c_1 t} \quad \text{and} \quad \|s_k(t) - s(t)\|_2 \leq \epsilon e^{c_1 t}.$$

Lastly, we remark that the initialization in Theorem 1 can be further relaxed to a wider basin of attraction around the symmetric initialization of interest. This follows from a similar argument as in Zucchet et al. (2025) who has studied the escape time from this initialization when $h = 1$.

Remark 1. *The initialization of interest is $s_k(0) \approx \frac{1}{T} \mathbf{1}_T$ for all $k \in [h]$ as seen in Figure 2. By expanding the dynamics around this initialization with $V_k \approx 0$ for all $k \in [h]$, we get:*

$$\dot{V}_k(0) \approx \frac{1}{T} \mathbf{G} \mathbf{1}_T, \quad \dot{s}_k(0) \approx 0.$$

Similarly, second-order local approximation shows that s_k has the largest increase towards the direction s_1^ . Therefore, we can quantify a wider basin of attraction for Theorem 1 as all V_k and s_k move towards the initialization space defined by Equation (5).*

3.3 Cooperation After Competition

In order to study the cooperative phase after the initial competitive phase, we consider the dynamics of the loss at various initializations around the fixed point in Equation (6). Consider the following initialization scheme:

$$\begin{aligned} V_1(0) = \dots = V_{h-1}(0) &\approx \frac{m_1^*}{h} V_1^*, & V_h(0) &\approx \frac{m_1^*}{h} V_1^*, \\ s_1(0) = \dots = s_{h-1}(0) &= s_1^*, & s_h &\approx s_1^*. \end{aligned} \quad (7)$$

The dynamics of s_1, \dots, s_{h-1} remain constant due to the projection. In addition, V_1, \dots, V_{h-1} are coupled due to the gradient flow. Therefore, the whole system collapses to the three equations, one for V that describes the ensemble and two V', s' that describes the offshooting head:

$$\begin{aligned}\dot{s}' &= \Pi(s')^2 (V'^\top \mathbf{G} - (h-1)\langle V', V \rangle s_1^* - \|V'\|^2 s'), \\ \dot{V} &= m_1^* \|s_1^*\|^2 V_1^* - (h-1)\|s_1^*\|^2 V - \langle s_1^*, s' \rangle V', \\ \dot{V}' &= \mathbf{G} s' - (h-1)\langle s_1^*, s' \rangle V - \|s'\|^2 V',\end{aligned}\tag{8}$$

We have a similar control to Theorem 2 for the dynamics of V, V' and s' . Theorem 3 establishes that the deviation from the cooperative system is bounded for a finite time that we can precisely control. This is due to a Lyapunov control argument where the norms of V and V' are bounded.

Theorem 3. *Assume that the following holds for $\epsilon \ll 1$:*

$$\begin{aligned}\forall k \in [h-1]: \|V(0) - V_k(0)\|_F \leq \epsilon, \|e_1 - s_k(0)\|_2 \leq \epsilon, \\ \text{and } \|V'(0) - V_h(0)\|_F \leq \epsilon, \|s'(0) - s_h(0)\|_2 \leq \epsilon.\end{aligned}$$

Let $\Delta(t)$ be the deviation from the cooperative system in Equation (8):

$$\begin{aligned}\Delta(t) = \max \left\{ \max_k \{ \|V_k(t) - V(t)\|_F, \|s_k(t) - s(t)\|_2 \}, \right. \\ \left. \|V_h(t) - V(t)\|_F, \|s_h(t) - s(t)\|_2 \right\}.\end{aligned}$$

Assuming that $\|s'(t) - s_1^*\| \geq \delta$ for all $t \in \mathbb{R}$, there exists a universal constant c_1 such that:

$$\Delta(t) \leq \epsilon e^{c_1 t}, \quad \forall t \in \left[0, \frac{1}{-c_1 \log \epsilon} \right].$$

The dynamics in Equation (8) is interesting as while V' grows in an orthogonal direction V_\perp to V_1^* , s' is still sparse around s_1^* . This is due to the fact that $\Pi(s') \approx 0$ at initialization as $s'(0) \approx s_1^*$ which leads to a scale separation between s' and \dot{V}' . Consequentially, when V' grows along some V_\perp , the prediction is pushed to include the unnecessary term, $V_\perp x_t$. However, this is instantly cancelled out by the progression of the ensemble, where V learns to offset this by learning $-V_\perp$. This collaborative behavior is best seen in our plots in Figure 10.

To simplify Equation (8), we show that the initialization in Equation (7) ensures that V is close to its optimal value, V^* , which is defined in Lemma 1. In fact, we can derive a precise statement about how far V is from V^* based on how much weight s' puts on the directions that are orthogonal to s_1^* :

Lemma 1. *Let $\Delta(t) = V(t) - V^*(t)$ where*

$$V^*(t) = \frac{1}{h-1} (m_1^* V_1^* - \langle s_1^*, s'(t) \rangle V'(t)).$$

Assuming that $\|s'(t) - s_1^*\| \geq \delta$ for all $t \in \mathbb{R}$, there exist constants $c_1(\delta), c_2$ such that

$$\|\Delta(t)\|_F \leq e^{-c_2 t} \|\Delta(0)\|_F + \frac{c_1(\delta)}{c_2}.$$

Inspired by Lemma 1 and numerical simulations, we approximate the full dynamics by a two-scale analysis where V is optimized faster, leading to the following dynamics:

$$\dot{V}' = \mathbf{G}_{(1)} s'_{(1)} - \|s'_{(1)}\|^2 V', \quad \dot{s}' = \Pi(s')^2 \left(V_{(1)}^\top \mathbf{G}_{(1)} - \|V'\|_F^2 s'_{(1)} \right),\tag{9}$$

where we introduce the following notation:

$$\mathbf{G}_{(i)} = \mathbf{G} - \sum_{j=1}^i m_j^* (V_j^* \otimes s_j^*), \quad V_{(i)} = V - \sum_{j=1}^i \langle V_j^*, V \rangle V_j^*, \quad s_{(i)} = s - \sum_{j=1}^i \langle s_j^*, s \rangle s_j^*.$$

We show that dynamics in Equation (9) converges to the second positional feature:

Theorem 4. Assume that the initialization verifies the following for all $k \in [2, h]$:

$$\langle V'(0), V_2^* \rangle \geq \langle V'(0), V_k^* \rangle \quad \langle s'(0), s_2^* \rangle \geq \langle s'(0), s_k^* \rangle.$$

Further, suppose that $V'(0), s'(0)$ are such that

$$\langle V'_{(1)}(0), \mathbf{G}_{(1)} s'_{(1)}(0) \rangle > \frac{1}{2} \|V'(0)\|_F^2 \|s'_{(1)}(0)\|^2. \quad (10)$$

Then, the dynamics of V' and s' converge to the following fixed point:

$$V'(\infty) = V_2^*, \quad s'(\infty) = s_2^*.$$

Theorem 4 is similar in nature to Theorem 1. Once there is an alignment to the second positional feature, the dynamics is such that the alignment is not broken. Notably, we require the initialization to satisfy Equation (10). This is to ensure that the dynamics start with an initial decrease on the loss beyond the first saddle point characterized in Theorem 4. Theorem 4 proves that a potential that characterizes the loss is monotonically minimized and this saddle is avoided. In Remark 2, we discuss how a small perturbation towards the second positional feature is sufficient to satisfy Equation (10).

Finally, in Section C.4, we extend our analysis to the specialization of an arbitrary head n after the system has acquired the first $n - 1$ features. Analogously to our previous derivation, we assume a single “free” head while the remainder of the ensemble is fixed at its optimal configuration. In contrast to the two-head case, we suppose that heads 2 through $n - 1$ have already specialized to positions 2 through $n - 1$, while all remaining heads, excluding the free one, retain the first feature and operate cooperatively with it.

4 Related Work

Our work is at the intersection of incremental learning, n -gram models and dynamics of attention.

Incremental learning. Plateau-like learning curves are a common feature in neural network training. Early analyses, such as Fukumizu & Amari (2000), attributed these behaviors to critical points in supervised learning. Subsequent studies have examined similar dynamics in a variety of simplified settings, including linear networks (Gissin et al., 2020; Saxe et al., 2019; Gidel et al., 2019; Arora et al., 2019; Jacot et al., 2021; Li et al., 2021; Razin et al., 2021; Jiang et al., 2022; Berthier, 2022; Pesme & Flammarion, 2023; Jin et al., 2023; Varre et al., 2023; 2024), ReLU models (Boursier et al., 2022; Abbe et al., 2023a), simplified transformer architectures (Boix-Adsera et al., 2023), and recent work argues for their universality (Ziyin et al., 2025; Kunin et al., 2025; Zhang et al., 2025a). In transformer training, plateaus followed by sudden capability gains (Chen et al., 2024a; Kim et al., 2024) are often observed in regression tasks (Garg et al., 2022; Von Oswald et al., 2023; Ahn et al., 2024), formal language recognition (Bhattamishra et al., 2023; Akyürek et al., 2024; D’Angelo et al., 2025; Cagnetta et al., 2025). Finally, Cagnetta & Wyart (2024); Cagnetta et al. (2025) study the effect of dataset size in learning random probabilistic context-free grammars, showing that the order of the learned hierarchy depends on data availability, a dynamic similar to the data-dependent stage progression in our observations.

n -gram models. n -gram language models (Jurafsky & Martin, 2009) serve as a toy setting to understand large language models. This perspective has motivated a range of studies: the optimization landscape has been characterized in Makuva et al. (2024), expressivity over n -gram distributions has been examined in Svete & Cotterell (2024) and sample complexity has been resolved in Yüksel & Flammarion (2025). Learning of variable-order n -grams have been studied by (Zhou et al., 2024) whereas (Deora et al., 2025) consider n -grams with different order. Connections between ICL and the emergence of induction heads (Elhage et al., 2021; Olsson et al., 2022), together with their acquisition via gradient descent (Nichani et al., 2024), are drawn by Bietti et al. (2023). Training dynamics on n -gram prediction tasks have also been shown to progress in stages: intermediate solutions approximate sub- n -grams (Edelman et al., 2024; Chen et al., 2024b), which later are formalized as near-stationary points by Varre et al. (2025). Despite leading to rich

phenomenology, n -grams are typically studied without any inherent hierarchical abstractions that are present in natural language (Wu et al., 2022; 2025). We also use a simplified synthetic data to isolate the phenomenon of study.

Dynamics of attention. The dynamics of attention have recently been explored through various simplified models. Specifically, (Snell et al., 2021) examine a “bag-of-words” proxy, while (Jelassi et al., 2022) investigate a simplified Vision Transformer (ViT) restricted to position-only attention. Under a masked language modeling objective, (Li et al., 2023) characterize a two-stage training regime. Further theoretical analyses include the stochastic gradient dynamics of position-free attention (Tian et al., 2023), the evolution of diagonal attention weights (Abbe et al., 2023b), and the behavior of linear attention within the framework of in-context linear regression (Zhang et al., 2025b). Particularly relevant to our data model, (Marion et al., 2025) study training trajectories in single-location regression, a setting related to sequence multi-index models (Cui et al., 2024; Troiani et al., 2025). Closest to our work, (Zucchet et al., 2025) consider the single-head case $h = 1$ and analyze the escape time from the initialization $V = 0, s = \frac{1}{T}\mathbf{1}_T$. While their analysis relies on a local Taylor approximation around this initialization, we characterize the full stage-wise saddle-to-saddle dynamics that emerge following the initial escape.

5 Conclusion

In this work, we introduce a simple yet theoretically rich task requiring transformers to implement multiple sparse attention patterns. We demonstrate that this task captures the core mechanics of position-dependent, incremental learning. Our analysis reveals a distinct phase transition: the dynamics begin in a competitive regime, where heads converge on the most statistically salient pattern, before transitioning into a cooperative regime characterized by head specialization. We formalize these observations through rigorous convergence results within a simplified regression framework that characterizes the underlying training dynamics. Our findings highlight the intricate interplay between attention sparsity and transformer learning dynamics—a connection that is fundamental to understanding how these models scale to complex reasoning and natural language processing tasks.

Acknowledgments

This project was supported by the Swiss National Science Foundation (grant number 212111) and an unrestricted gift from Google.

References

- Emmanuel Abbe, Enric Boix Adsera, and Theodor Misiakiewicz. Sgd learning on neural networks: leap complexity and saddle-to-saddle dynamics. In *The Thirty Sixth Annual Conference on Learning Theory*, pp. 2552–2623. PMLR, 2023a.
- Emmanuel Abbe, Samy Bengio, Enric Boix-Adserà, Etai Littwin, and Joshua M. Susskind. Transformers learn through gradual rank increase. In Alice Oh, Tristan Naumann, Amir Globerson, Kate Saenko, Moritz Hardt, and Sergey Levine (eds.), *Advances in Neural Information Processing Systems 36: Annual Conference on Neural Information Processing Systems 2023, NeurIPS 2023, New Orleans, LA, USA, December 10 - 16, 2023*, 2023b. URL http://papers.nips.cc/paper_files/paper/2023/hash/4d69c1c057a8bd570ba4a7b71aae8331-Abstract-Conference.html.
- Kwangjun Ahn, Xiang Cheng, Hadi Daneshmand, and Suvrit Sra. Transformers learn to implement preconditioned gradient descent for in-context learning. *Advances in Neural Information Processing Systems*, 36, 2024.
- Ekin Akyürek, Bailin Wang, Yoon Kim, and Jacob Andreas. In-context language learning: Architectures and algorithms. *arXiv preprint arXiv:2401.12973*, 2024.

- Sanjeev Arora, Nadav Cohen, Wei Hu, and Yuping Luo. Implicit regularization in deep matrix factorization. *Advances in Neural Information Processing Systems*, 32, 2019.
- Raphaël Berthier. Incremental learning in diagonal linear networks. *arXiv preprint arXiv:2208.14673*, 2022.
- Satwik Bhattamishra, Arkil Patel, Phil Blunsom, and Varun Kanade. Understanding in-context learning in transformers and llms by learning to learn discrete functions. *arXiv preprint arXiv:2310.03016*, 2023.
- Alberto Bietti, Vivien Cabannes, Diane Bouchacourt, Hervé Jégou, and Léon Bottou. Birth of a transformer: A memory viewpoint. In Alice Oh, Tristan Naumann, Amir Globerson, Kate Saenko, Moritz Hardt, and Sergey Levine (eds.), *Advances in Neural Information Processing Systems 36: Annual Conference on Neural Information Processing Systems 2023, NeurIPS 2023, New Orleans, LA, USA, December 10 - 16, 2023*, 2023. URL http://papers.nips.cc/paper_files/paper/2023/hash/0561738a239a995c8cd2ef0e50cfa4fd-Abstract-Conference.html.
- Enric Boix-Adsera, Etai Littwin, Emmanuel Abbe, Samy Bengio, and Joshua Susskind. Transformers learn through gradual rank increase. *arXiv preprint arXiv:2306.07042*, 2023.
- Etienne Boursier, Loucas Pillaud-Vivien, and Nicolas Flammarion. Gradient flow dynamics of shallow reLU networks for square loss and orthogonal inputs. In Alice H. Oh, Alekh Agarwal, Danielle Belgrave, and Kyunghyun Cho (eds.), *Advances in Neural Information Processing Systems*, 2022. URL <https://openreview.net/forum?id=L74c-iUxQ1I>.
- Tom B. Brown, Benjamin Mann, Nick Ryder, Melanie Subbiah, Jared Kaplan, Prafulla Dhariwal, Arvind Neelakantan, Pranav Shyam, Girish Sastry, Amanda Askell, Sandhini Agarwal, Ariel Herbert-Voss, Gretchen Krueger, Tom Henighan, Rewon Child, Aditya Ramesh, Daniel M. Ziegler, Jeffrey Wu, Clemens Winter, Christopher Hesse, Mark Chen, Eric Sigler, Mateusz Litwin, Scott Gray, Benjamin Chess, Jack Clark, Christopher Berner, Sam McCandlish, Alec Radford, Ilya Sutskever, and Dario Amodei. Language models are few-shot learners. In Hugo Larochelle, Marc’Aurelio Ranzato, Raia Hadsell, Maria-Florina Balcan, and Hsuan-Tien Lin (eds.), *Advances in Neural Information Processing Systems 33: Annual Conference on Neural Information Processing Systems 2020, NeurIPS 2020, December 6-12, 2020, virtual*, 2020. URL <https://proceedings.neurips.cc/paper/2020/hash/1457c0d6bfc4967418bfb8ac142f64a-Abstract.html>.
- Francesco Cagnetta and Matthieu Wyart. Towards a theory of how the structure of language is acquired by deep neural networks. In Amir Globersons, Lester Mackey, Danielle Belgrave, Angela Fan, Ulrich Paquet, Jakub M. Tomczak, and Cheng Zhang (eds.), *Advances in Neural Information Processing Systems 38: Annual Conference on Neural Information Processing Systems 2024, NeurIPS 2024, Vancouver, BC, Canada, December 10 - 15, 2024*, 2024. URL http://papers.nips.cc/paper_files/paper/2024/hash/9740da1c07c7b451af14e11523f95271-Abstract-Conference.html.
- Francesco Cagnetta, Hyunmo Kang, and Matthieu Wyart. Learning curves theory for hierarchically compositional data with power-law distributed features. In *Forty-second International Conference on Machine Learning, ICML 2025, Vancouver, BC, Canada, July 13-19, 2025*. OpenReview.net, 2025. URL <https://openreview.net/forum?id=Lw0kC75dY0>.
- Angelica Chen, Ravid Shwartz-Ziv, Kyunghyun Cho, Matthew L. Leavitt, and Naomi Saphra. Sudden drops in the loss: Syntax acquisition, phase transitions, and simplicity bias in mlms. In *The Twelfth International Conference on Learning Representations, ICLR 2024, Vienna, Austria, May 7-11, 2024*. OpenReview.net, 2024a. URL <https://openreview.net/forum?id=M05PiKHELW>.
- Siyu Chen, Heejune Sheen, Tianhao Wang, and Zhuoran Yang. Unveiling induction heads: Provable training dynamics and feature learning in transformers. In *The Thirty-eighth Annual Conference on Neural Information Processing Systems*, 2024b.
- Hugo Cui, Freya Behrens, Florent Krzakala, and Lenka Zdeborová. A phase transition between positional and semantic learning in a solvable model of dot-product attention. In Amir Globersons, Lester Mackey, Danielle Belgrave, Angela Fan, Ulrich Paquet, Jakub M. Tomczak, and Cheng Zhang (eds.), *Advances in Neural Information Processing Systems 38: Annual Conference on Neural Information Processing Systems 2024*,

- NeurIPS 2024, Vancouver, BC, Canada, December 10 - 15, 2024*, 2024. URL http://papers.nips.cc/paper_files/paper/2024/hash/3fefebc2d4e3c1c6ee9b892bd293117d-Abstract-Conference.html.
- Francesco D’Angelo, Francesco Croce, and Nicolas Flammarion. Selective induction heads: How transformers select causal structures in context. In *The Thirteenth International Conference on Learning Representations, ICLR 2025, Singapore, April 24-28, 2025*. OpenReview.net, 2025. URL <https://openreview.net/forum?id=bnJgzaQjWf>.
- Puneesh Deora, Bhavya Vasudeva, Tina Behnia, and Christos Thrampoulidis. In-context occam’s razor: How transformers prefer simpler hypotheses on the fly. *CoRR*, abs/2506.19351, 2025. doi: 10.48550/ARXIV.2506.19351. URL <https://doi.org/10.48550/arXiv.2506.19351>.
- Benjamin L Edelman, Ezra Edelman, Surbhi Goel, Eran Malach, and Nikolaos Tsilivis. The evolution of statistical induction heads: In-context learning markov chains. *arXiv preprint arXiv:2402.11004*, 2024.
- Nelson Elhage, Neel Nanda, Catherine Olsson, Tom Henighan, Nicholas Joseph, Ben Mann, Amanda Askell, Yuntao Bai, Anna Chen, Tom Conerly, et al. A mathematical framework for transformer circuits. *Transformer Circuits Thread*, 1(1):12, 2021.
- K. Fukumizu and S. Amari. Local minima and plateaus in hierarchical structures of multilayer perceptrons. *Neural Networks*, 13(3):317–327, 2000. ISSN 0893-6080. doi: [https://doi.org/10.1016/S0893-6080\(00\)00009-5](https://doi.org/10.1016/S0893-6080(00)00009-5). URL <https://www.sciencedirect.com/science/article/pii/S0893608000000095>.
- Shivam Garg, Dimitris Tsipras, Percy S Liang, and Gregory Valiant. What can transformers learn in-context? a case study of simple function classes. *Advances in Neural Information Processing Systems*, 35:30583–30598, 2022.
- Gauthier Gidel, Francis Bach, and Simon Lacoste-Julien. Implicit regularization of discrete gradient dynamics in linear neural networks. *Advances in Neural Information Processing Systems*, 32, 2019.
- Daniel Gissin, Shai Shalev-Shwartz, and Amit Daniely. The implicit bias of depth: How incremental learning drives generalization. In *International Conference on Learning Representations*, 2020.
- Arthur Jacot, François Ged, Berfin Şimşek, Clément Hongler, and Franck Gabriel. Saddle-to-saddle dynamics in deep linear networks: Small initialization training, symmetry, and sparsity. *arXiv preprint arXiv:2106.15933*, 2021.
- Samy Jelassi, Michael E. Sander, and Yuanzhi Li. Vision transformers provably learn spatial structure. In Sanmi Koyejo, S. Mohamed, A. Agarwal, Danielle Belgrave, K. Cho, and A. Oh (eds.), *Advances in Neural Information Processing Systems 35: Annual Conference on Neural Information Processing Systems 2022, NeurIPS 2022, New Orleans, LA, USA, November 28 - December 9, 2022*, 2022. URL http://papers.nips.cc/paper_files/paper/2022/hash/f69707de866eb0805683d3521756b73f-Abstract-Conference.html.
- Liwei Jiang, Yudong Chen, and Lijun Ding. Algorithmic regularization in model-free overparametrized asymmetric matrix factorization. *arXiv preprint arXiv:2203.02839*, 2022.
- Jikai Jin, Zhiyuan Li, Kaifeng Lyu, Simon S Du, and Jason D Lee. Understanding incremental learning of gradient descent: A fine-grained analysis of matrix sensing. *arXiv preprint arXiv:2301.11500*, 2023.
- Daniel Jurafsky and James H. Martin. *Speech and Language Processing: An Introduction to Natural Language Processing, Computational Linguistics, and Speech Recognition*. Prentice Hall, Upper Saddle River, NJ, 2nd edition, 2009.
- Jaeyeon Kim, Sehyun Kwon, Joo Young Choi, Jongho Park, Jaewoong Cho, Jason D. Lee, and Ernest K. Ryu. Task diversity shortens the icl plateau, 2024. URL <https://arxiv.org/abs/2410.05448>.
- Daniel Kunin, Giovanni Luca Marchetti, Feng Chen, Dhruva Karkada, James B. Simon, Michael Robert DeWeese, Surya Ganguli, and Nina Miolane. Alternating gradient flows: A theory of feature learning in two-layer neural networks. *CoRR*, abs/2506.06489, 2025. doi: 10.48550/ARXIV.2506.06489. URL <https://doi.org/10.48550/arXiv.2506.06489>.

- Yuchen Li, Yuanzhi Li, and Andrej Risteski. How do transformers learn topic structure: Towards a mechanistic understanding. In Andreas Krause, Emma Brunskill, Kyunghyun Cho, Barbara Engelhardt, Sivan Sabato, and Jonathan Scarlett (eds.), *International Conference on Machine Learning, ICML 2023, 23-29 July 2023, Honolulu, Hawaii, USA*, volume 202 of *Proceedings of Machine Learning Research*, pp. 19689–19729. PMLR, 2023. URL <https://proceedings.mlr.press/v202/li23p.html>.
- Zhiyuan Li, Yuping Luo, and Kaifeng Lyu. Towards resolving the implicit bias of gradient descent for matrix factorization: Greedy low-rank learning. In *International Conference on Learning Representations*, 2021.
- Ashok Vardhan Makkuva, Marco Bondaschi, Adway Girish, Alliot Nagle, Martin Jaggi, Hyeji Kim, and Michael Gastpar. Attention with markov: A framework for principled analysis of transformers via markov chains. *arXiv preprint arXiv:2402.04161*, 2024.
- Pierre Marion, Raphaël Berthier, Gérard Biau, and Claire Boyer. Attention layers provably solve single-location regression. In *The Thirteenth International Conference on Learning Representations, ICLR 2025, Singapore, April 24-28, 2025*. OpenReview.net, 2025. URL <https://openreview.net/forum?id=DV1Pp7Jd7P>.
- Eshaan Nichani, Alex Damian, and Jason D. Lee. How transformers learn causal structure with gradient descent, 2024. URL <https://arxiv.org/abs/2402.14735>.
- Catherine Olsson, Nelson Elhage, Neel Nanda, Nicholas Joseph, Nova DasSarma, Tom Henighan, Ben Mann, Amanda Askell, Yuntao Bai, Anna Chen, Tom Conerly, Dawn Drain, Deep Ganguli, Zac Hatfield-Dodds, Danny Hernandez, Scott Johnston, Andy Jones, Jackson Kernion, Liane Lovitt, Kamal Ndousse, Dario Amodei, Tom Brown, Jack Clark, Jared Kaplan, Sam McCandlish, and Chris Olah. In-context learning and induction heads. *CoRR*, abs/2209.11895, 2022. doi: 10.48550/ARXIV.2209.11895. URL <https://doi.org/10.48550/arXiv.2209.11895>.
- Scott Pesme and Nicolas Flammarion. Saddle-to-saddle dynamics in diagonal linear networks. *Advances in Neural Information Processing Systems*, 36:7475–7505, 2023.
- Noam Razin, Asaf Maman, and Nadav Cohen. Implicit regularization in tensor factorization. *CoRR*, abs/2102.09972, 2021. URL <https://arxiv.org/abs/2102.09972>.
- Andrew M Saxe, James L McClelland, and Surya Ganguli. A mathematical theory of semantic development in deep neural networks. *Proceedings of the National Academy of Sciences*, 116(23):11537–11546, 2019.
- Charlie Snell, Ruiqi Zhong, Dan Klein, and Jacob Steinhardt. Approximating how single head attention learns. *CoRR*, abs/2103.07601, 2021. URL <https://arxiv.org/abs/2103.07601>.
- Anej Svete and Ryan Cotterell. Transformers can represent n -gram language models. *arXiv preprint arXiv:2404.14994*, 2024.
- Yuandong Tian, Yiping Wang, Beidi Chen, and Simon S. Du. Scan and snap: Understanding training dynamics and token composition in 1-layer transformer. In Alice Oh, Tristan Naumann, Amir Globerson, Kate Saenko, Moritz Hardt, and Sergey Levine (eds.), *Advances in Neural Information Processing Systems 36: Annual Conference on Neural Information Processing Systems 2023, NeurIPS 2023, New Orleans, LA, USA, December 10 - 16, 2023*, 2023. URL http://papers.nips.cc/paper_files/paper/2023/hash/e359e56ba306b674e8952349c6049e-Abstract-Conference.html.
- Emanuele Troiani, Hugo Cui, Yatin Dandi, Florent Krzakala, and Lenka Zdeborová. Fundamental limits of learning in sequence multi-index models and deep attention networks: high-dimensional asymptotics and sharp thresholds. In Aarti Singh, Maryam Fazel, Daniel Hsu, Simon Lacoste-Julien, Felix Berkenkamp, Tegan Maharaj, Kiri Wagstaff, and Jerry Zhu (eds.), *Forty-second International Conference on Machine Learning, ICML 2025, Vancouver, BC, Canada, July 13-19, 2025*, volume 267 of *Proceedings of Machine Learning Research*. PMLR / OpenReview.net, 2025. URL <https://proceedings.mlr.press/v267/troiani25a.html>.
- Aditya Varre, Gizem Yüce, and Nicolas Flammarion. Learning in-context n -grams with transformers: Sub- n -grams are near-stationary points. In *International Conference on Machine Learning*, 2025.

- Aditya Vardhan Varre, Maria-Luiza Vladarean, Loucas Pillaud-Vivien, and Nicolas Flammarion. On the spectral bias of two-layer linear networks. In *Thirty-seventh Conference on Neural Information Processing Systems*, 2023. URL <https://openreview.net/forum?id=FFdrXkm3Cz>.
- Aditya Vardhan Varre, Margarita Sagitova, and Nicolas Flammarion. Sgd vs gd: Rank deficiency in linear networks. *Advances in Neural Information Processing Systems*, 37:60133–60161, 2024.
- Johannes Von Oswald, Eyvind Niklasson, Ettore Randazzo, João Sacramento, Alexander Mordvintsev, Andrey Zhmoginov, and Max Vladymyrov. Transformers learn in-context by gradient descent. In *International Conference on Machine Learning*, pp. 35151–35174. PMLR, 2023.
- Shuchen Wu, Noémi Élteto, Ishita Dasgupta, and Eric Schulz. Learning structure from the ground up - hierarchical representation learning by chunking. In Sanmi Koyejo, S. Mohamed, A. Agarwal, Danielle Belgrave, K. Cho, and A. Oh (eds.), *Advances in Neural Information Processing Systems 35: Annual Conference on Neural Information Processing Systems 2022, NeurIPS 2022, New Orleans, LA, USA, November 28 - December 9, 2022*, 2022. URL http://papers.nips.cc/paper_files/paper/2022/hash/ee5bb72130c332c3d4bf8d231e617506-Abstract-Conference.html.
- Shuchen Wu, Mirko Thalmann, Peter Dayan, Zeynep Akata, and Eric Schulz. Building, reusing, and generalizing abstract representations from concrete sequences. In *The Thirteenth International Conference on Learning Representations, ICLR 2025, Singapore, April 24-28, 2025*. OpenReview.net, 2025. URL <https://openreview.net/forum?id=xIUUnzrUtD>.
- Oğuz Kaan Yüksel and Nicolas Flammarion. On the sample complexity of next-token prediction. In *The 28th International Conference on Artificial Intelligence and Statistics*, 2025. URL <https://openreview.net/forum?id=eJkNMwzZzy>.
- Oğuz Kaan Yüksel, Mathieu Even, and Nicolas Flammarion. Long-context linear system identification. In *The Thirteenth International Conference on Learning Representations, ICLR 2025, Singapore, April 24-28, 2025*. OpenReview.net, 2025. URL <https://openreview.net/forum?id=2TuUXtLGhT>.
- Yedi Zhang, Andrew Saxe, and Peter E Latham. Saddle-to-saddle dynamics explains a simplicity bias across neural network architectures. *arXiv preprint arXiv:2512.20607*, 2025a.
- Yedi Zhang, Aaditya K. Singh, Peter E. Latham, and Andrew M. Saxe. Training dynamics of in-context learning in linear attention. In *Forty-second International Conference on Machine Learning, ICML 2025, Vancouver, BC, Canada, July 13-19, 2025*. OpenReview.net, 2025b. URL <https://openreview.net/forum?id=aFNq67ilos>.
- Ruida Zhou, Chao Tian, and Suhas N. Diggavi. Transformers learn variable-order markov chains in-context. *CoRR*, abs/2410.05493, 2024. doi: 10.48550/ARXIV.2410.05493. URL <https://doi.org/10.48550/arXiv.2410.05493>.
- Liu Ziyin, Yizhou Xu, Tomaso Poggio, and Isaac Chuang. Parameter symmetry potentially unifies deep learning theory. *arXiv preprint arXiv:2502.05300*, 2025.
- Nicolas Zucchet, Francesco D’Angelo, Andrew K. Lampinen, and Stephanie C. Y. Chan. The emergence of sparse attention: impact of data distribution and benefits of repetition. *CoRR*, abs/2505.17863, 2025. doi: 10.48550/ARXIV.2505.17863. URL <https://doi.org/10.48550/arXiv.2505.17863>.

Organization of the Appendix

The appendix is organized as follows,

- Appendix A provides the experimental details.
- Appendix B presents additional experiments.
- Appendix C provide proofs of the theoretical results.
- Appendix D discusses how the initialization in our main theorems can be relaxed.

Appendix A Experimental Details

The full model has a standard single-layer transformer decoder architecture as discussed in Section 2.2. It uses absolute positional encodings with learnable embedding and unembedding matrices and has the configuration shown in Table 3. The minimal model, as described in Section 2.3, removes layer normalization, dropout, residual connections, key and output attention matrices and the MLP layer. It uses one-hot positional encodings and does not have embedding and unembedding matrices. Both the full model and the minimal model are trained with the same optimization hyperparameters listed in Table 2, and the same synthetic data generation process described in Table 1. The main difference in the learning task between the two models is the interval lengths $|I(k)|$ of the Markov process: the full model uses intervals of length 4, while the minimal model uses intervals of length 2, as summarized in Table 4.

We train the n -gram models using the same architecture and optimization hyperparameters as the full transformer model but training with windows of size n sliding over the full sequence. The source code to reproduce our experiments is available at <https://github.com/ralvarezlucend/IL-SAP-Transformers>.

Table 1: Synthetic dataset parameters

Parameter	Value
Heads h	3
Dictionary size d	50
Multiplicative constant m	1.7
Base scale b_0	10
Sequence length T	20
Train samples	9000
Test samples	3000
Seed	0

Table 2: Optimization hyperparameters

Parameter	Value
Steps	2000
Batch size	3000
Gradient clipping	1.0
Optimizer	AdamW
Weight decay	0.01
Learning rate	0.003
Scheduler	ReduceLROnPlateau
Patience	10
Factor	0.5

Table 3: Transformer configuration

Parameter	Value
Hidden dimension	255
Feedforward dimension	64
Dropout	0.1
Initialization scale	1
Number of blocks	1
Number of heads	3

Table 4: Markov process intervals

	Full	Minimal
w	12	6
$I(1)$	{1, 2, 3, 4}	{1, 2}
$I(2)$	{5, 6, 7, 8}	{3, 4}
$I(3)$	{9, 10, 11, 12}	{5, 6}

Appendix B Additional Experiments

We run additional experiments to study incremental learning behavior under different settings. In particular, we study the effect of infinite data versus finite data, different orders of importance with non-uniform interval lengths and the impact of weight decay.

B.1 Infinite Data

Instead of training on a finite dataset of 9000 samples, we train the model with infinite data by sampling a new batch of data at each step. This removes any effect of overfitting in incremental learning. We observe in Figure 6 and Figure 7 that the model still exhibits the same behavior. This experiment is run with the minimal architecture described in Section 2.4.

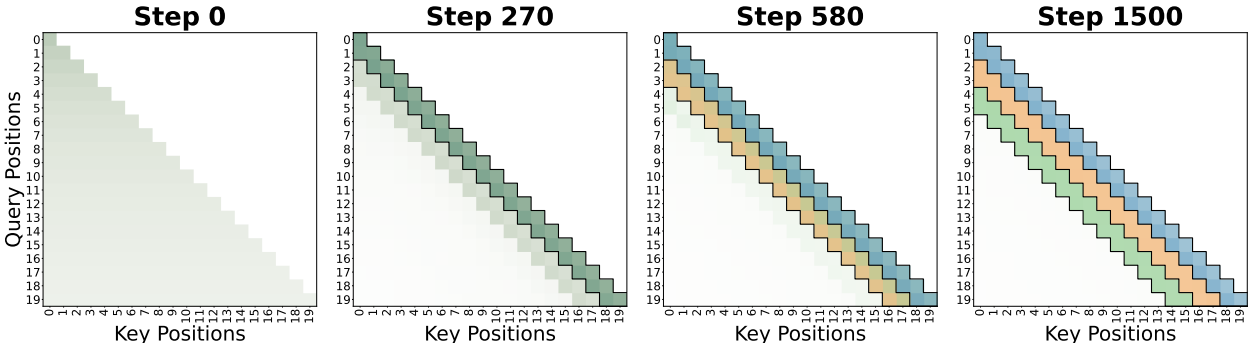


Figure 6: Attention patterns over the training steps with online sampling of data.

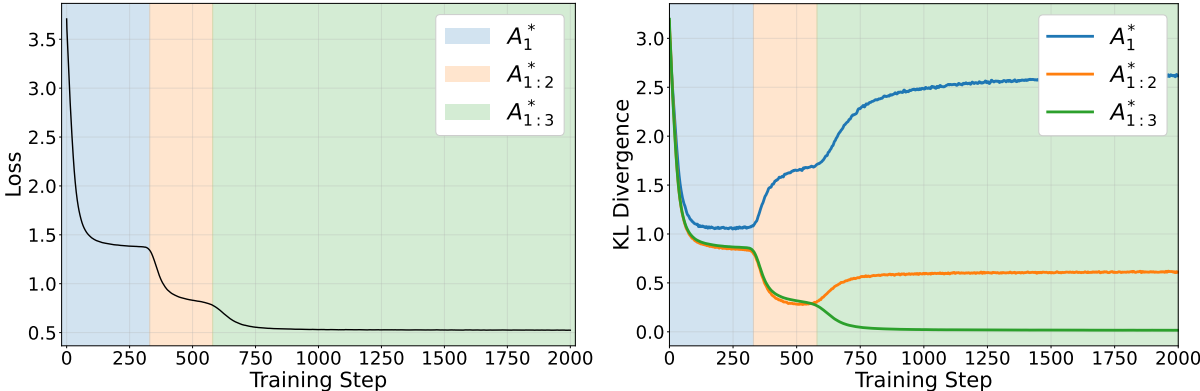


Figure 7: Validation loss and KL divergence over the training steps with online sampling of data.

B.2 Reverse Order

We reverse the order of importance of the intervals such that the most important interval is the furthest one. Figure 8 and Figure 9 show the results when $I(3) = \{12, 13\}$, $I(2) = \{8, 9, 10, 11\}$ and $I(1) = \{0, 1, 2, 3, 4, 5, 6, 7\}$ which reveals the same behavior as the original order. We also note that it is generally easier to observe incremental learning behaviour when the most important interval is the furthest one. This indicates that the learning dynamics is impacted by the sequential structure of the task. This experiment is run with the full architecture described in Section 2.2.

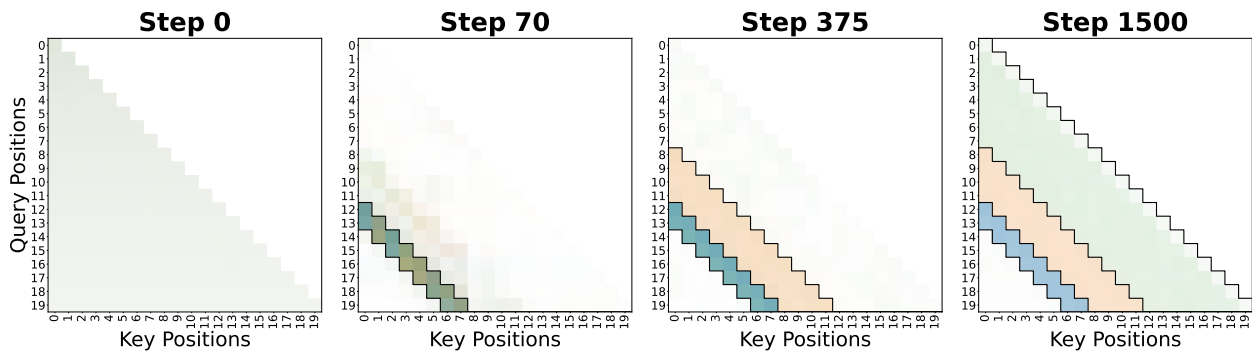


Figure 8: Attention patterns over the training steps with reversed order of importance and varying interval lengths.

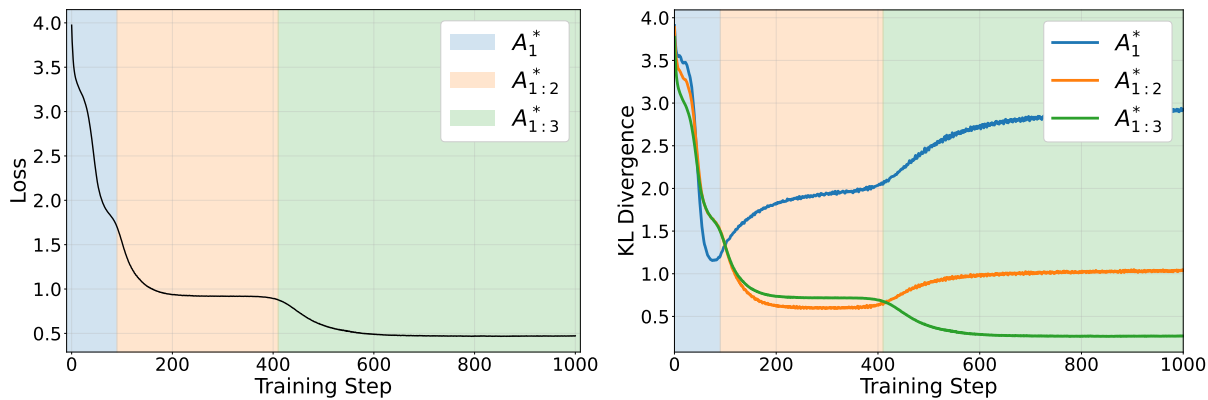


Figure 9: Validation loss and KL divergence over the training steps with reversed order of importance and varying interval lengths.

B.3 Weight Decay

We also study the impact of weight decay on the learning dynamics. We observe almost no difference in the learning dynamics when weight decay is not applied so we do not report the results.

B.4 Simulations

We present numerical simulations of the gradient flow dynamics of the loss in Equation (4) with the following parameters: $d = 50$, $T = 40$, $h = 3$, $|I(k)| = 1$ for all $k \in [h]$, $m = 1.7$, $\lambda = 0$. We initialize the value parameters V_i to 0 and the attention patterns s_i to $\frac{1}{T}1_T + \epsilon_i$ where ϵ_i are sampled from Gaussian distribution with zero-mean and ϵI_T covariance with $\epsilon = 10^{-6}$. Figure 10 shows the evolution of the attention patterns s_k , the value parameters V_k and the loss over time.

The results aligns with the transformer experiments in Section 2.2. Similar to the transformer experiments, the heads first learn from the position (1) and then the position (2) and finally the position (3). The time scales of these stages are clearly separated where the first stage is the fastest and the third stage is the slowest. Notably, at first, all heads tries to learn from the position (1) as it is related to the most important feature. After this competition phase, the heads start to learn from the position (2) and then the position (3) where they specialize in different patterns. Here, they cooperate to learn from the position (3). In particular, the first head offsets feature (3) as the third head’s residual attention on the first position results in a cross term.

B.5 Two-block Transformers

We train 2-block minimal and full transformers with the same configuration as in Appendix A but adjusting the learning rate and number of training examples. Figures 11 and 12 shows that the incremental learning behavior is similar to the 1-block case. We observe that the first region corresponding to first feature matrix is less pronounced.

B.6 Non-uniform α values

We run experiments with $\alpha = [0.7, 0.3]$ in Figure 13 and observe that the model still exhibits incremental learning. In Figure 14, we observe the checkered pattern where heads focus more attention on the position with the highest α value.

B.7 Overlapping Intervals

We run experiments with overlapping intervals where $I(1) = \{5, 6, 7, 8\}$, $I(2) = \{3, 4, 5, 6\}$, and $I(3) = \{1, 2, 3, 4\}$. This is interval lengths of 4 with an overlap or stride of 2. We try learning transformers with three or four heads. We observe in Figure 15 that the model with four heads still exhibits incremental learning behavior. Similar results are observed for the model with three heads and thus omitted. Attention patterns in Figures 16 and 17 reveal the different ordering of learnings for three and four heads. When the intervals are overlapping, it is unclear which positions are statistically the most significant and transformers may follow different solutions based on feature matrices.

B.8 Stochastic Gradient Descent (SGD)

We run experiments with SGD optimizer instead of AdamW. We observe in Figure 18 and Figure 19 that the quantitative behavior of incremental learning is same.

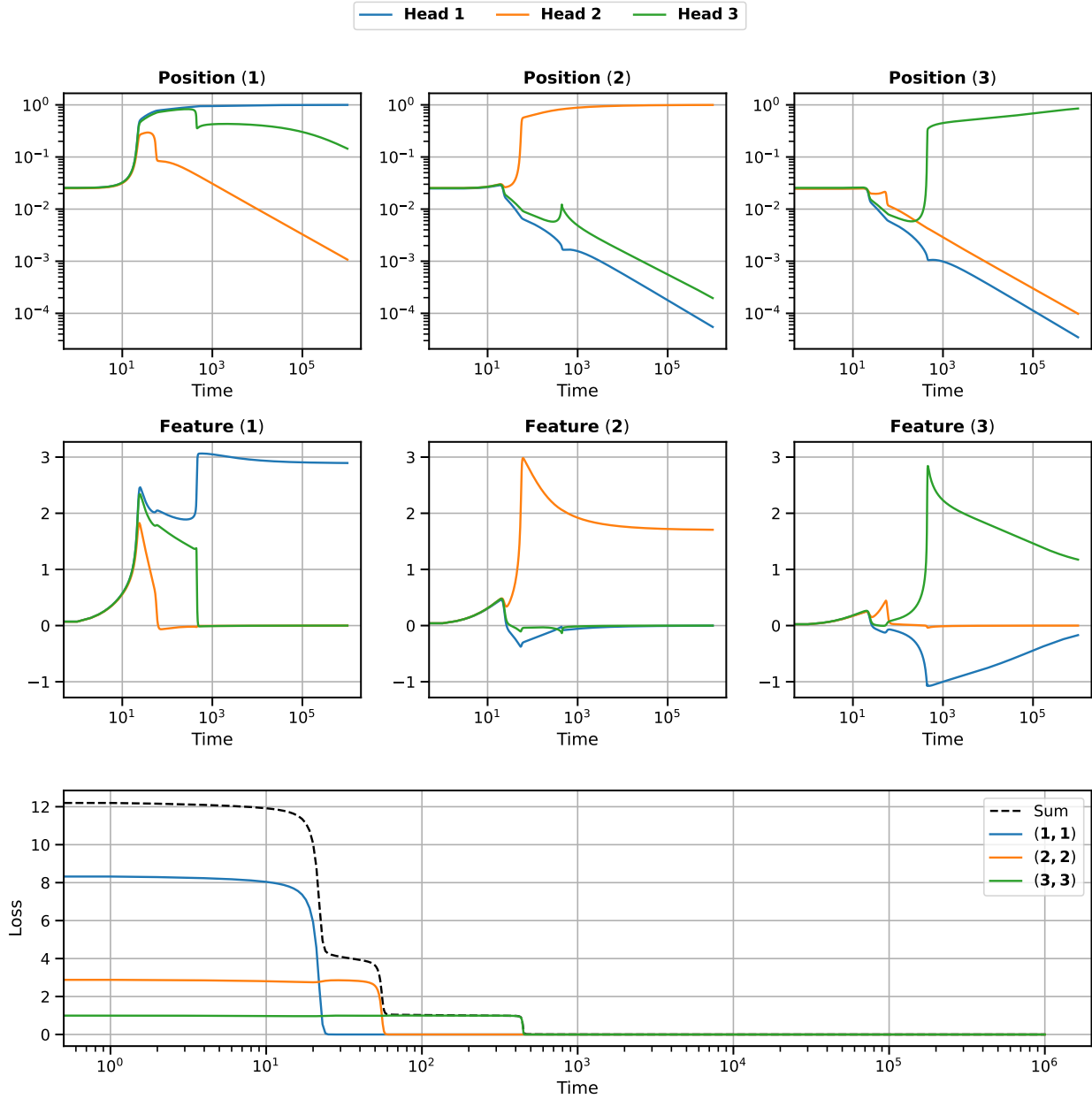


Figure 10: (Top) The evolution of the attention patterns s_k over time. (Middle) The evolution of the value parameters V_k over time. We only plot the relevant coordinates of s_k and V_k for clarity. (Bottom) The evolution of the loss over time. We decompose the loss into the (feature, position) contributions which are plotted in the color of the heads that learn these contributions.

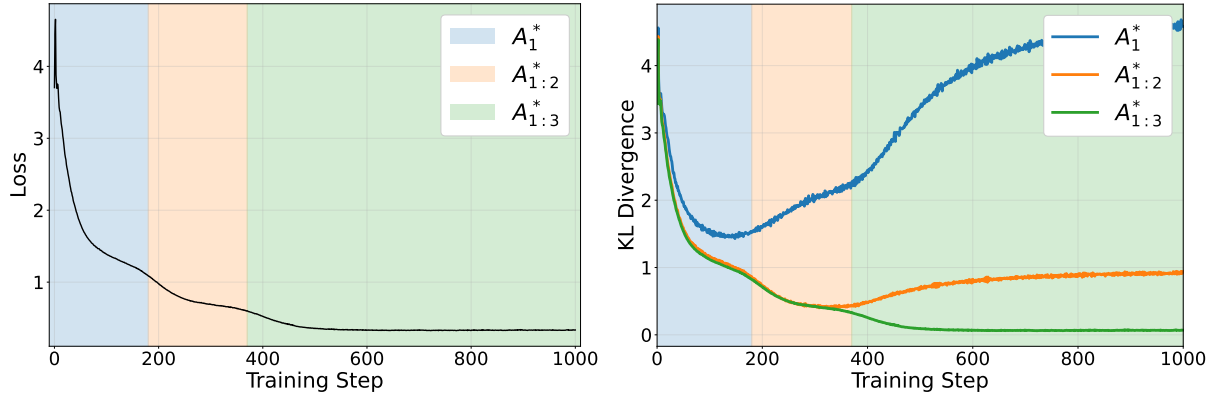


Figure 11: Validation loss and KL divergence over the training steps for a 2-layer minimal transformer.

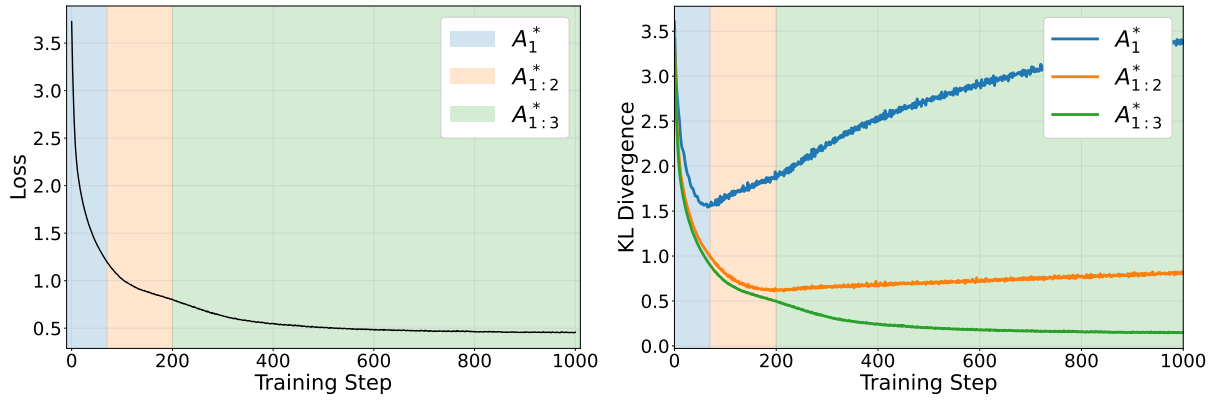


Figure 12: Validation loss and KL divergence over the training steps for a 2-layer full transformer.

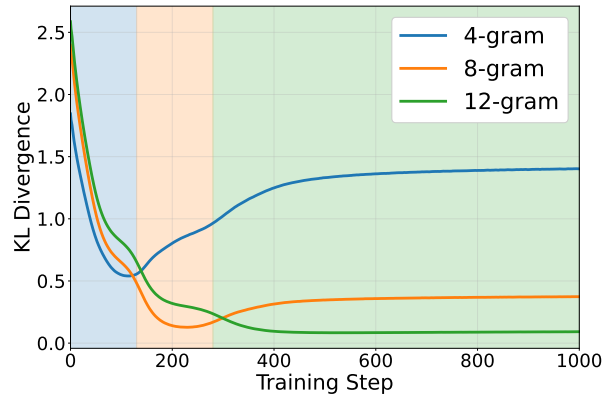


Figure 13: KL divergence over the training steps with non-uniform α values.

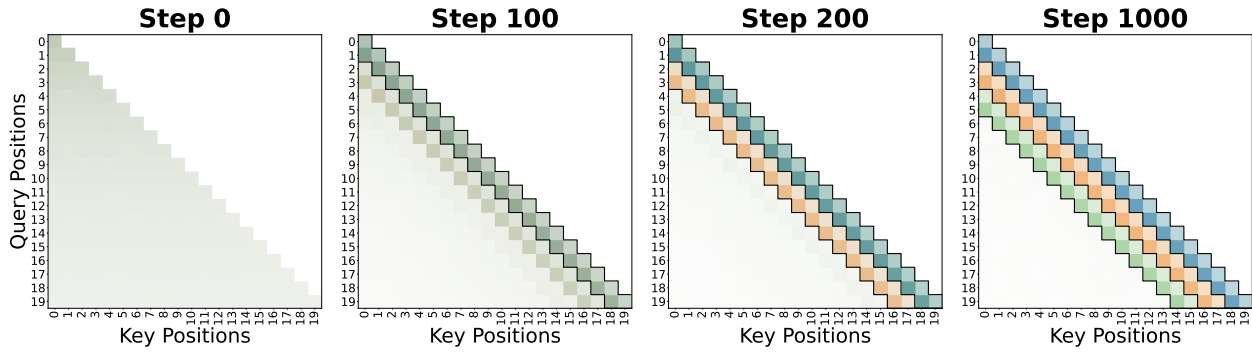


Figure 14: Attention patterns over the training steps with non-uniform α values.

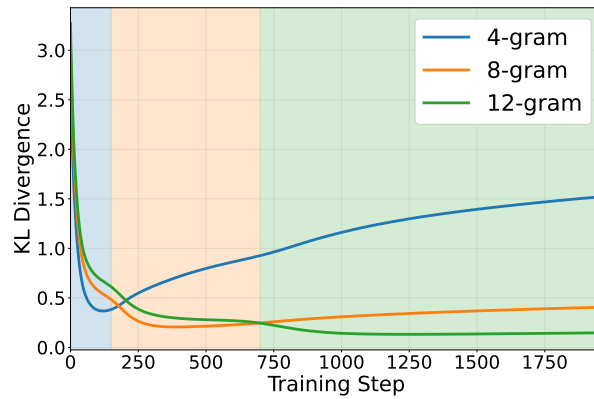


Figure 15: KL divergence over the training steps with intervals of size 4 and overlap of 2 for a transformer model with 4 heads.

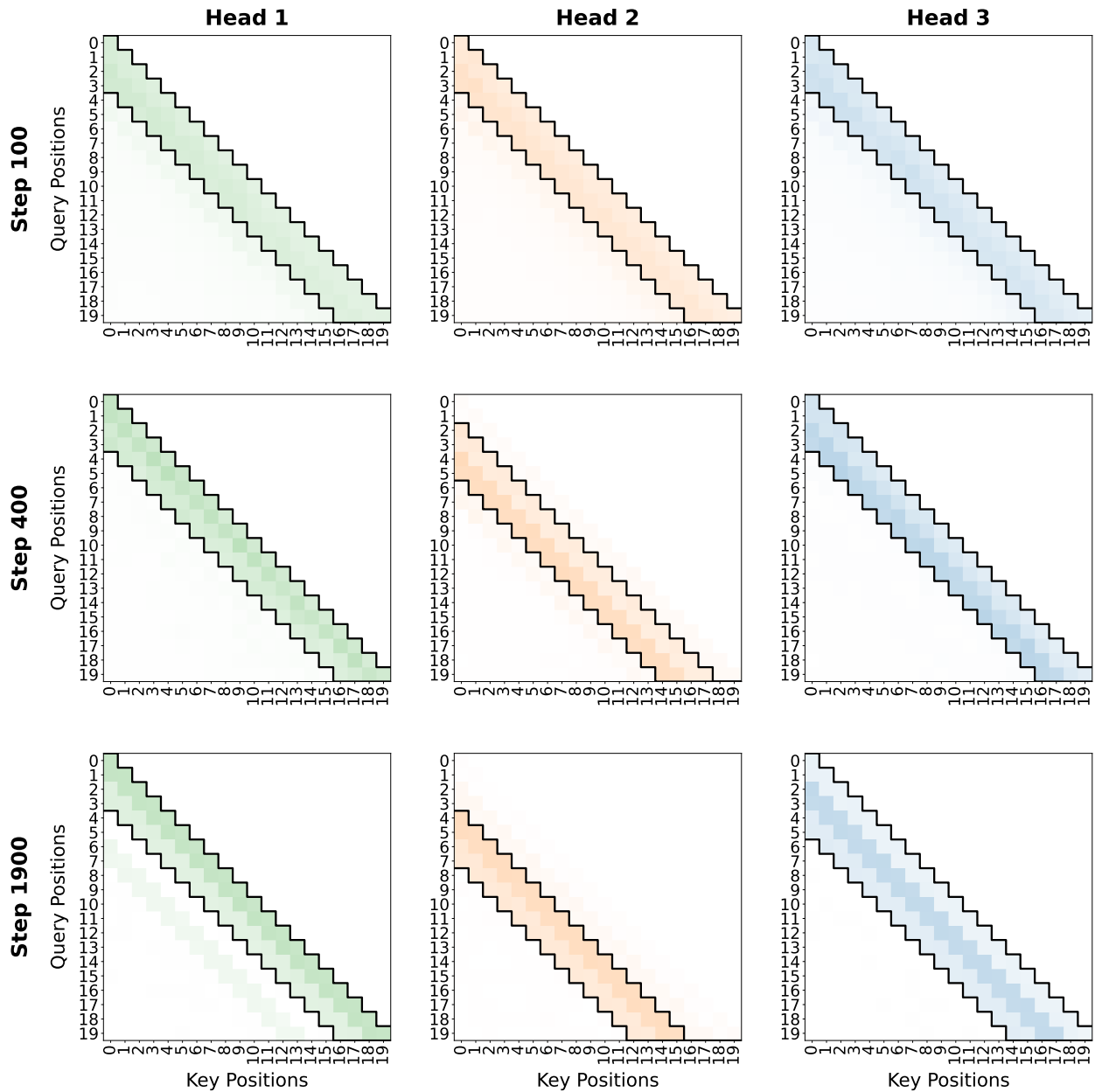


Figure 16: Attention patterns for 3 heads over the training steps with overlapping intervals.

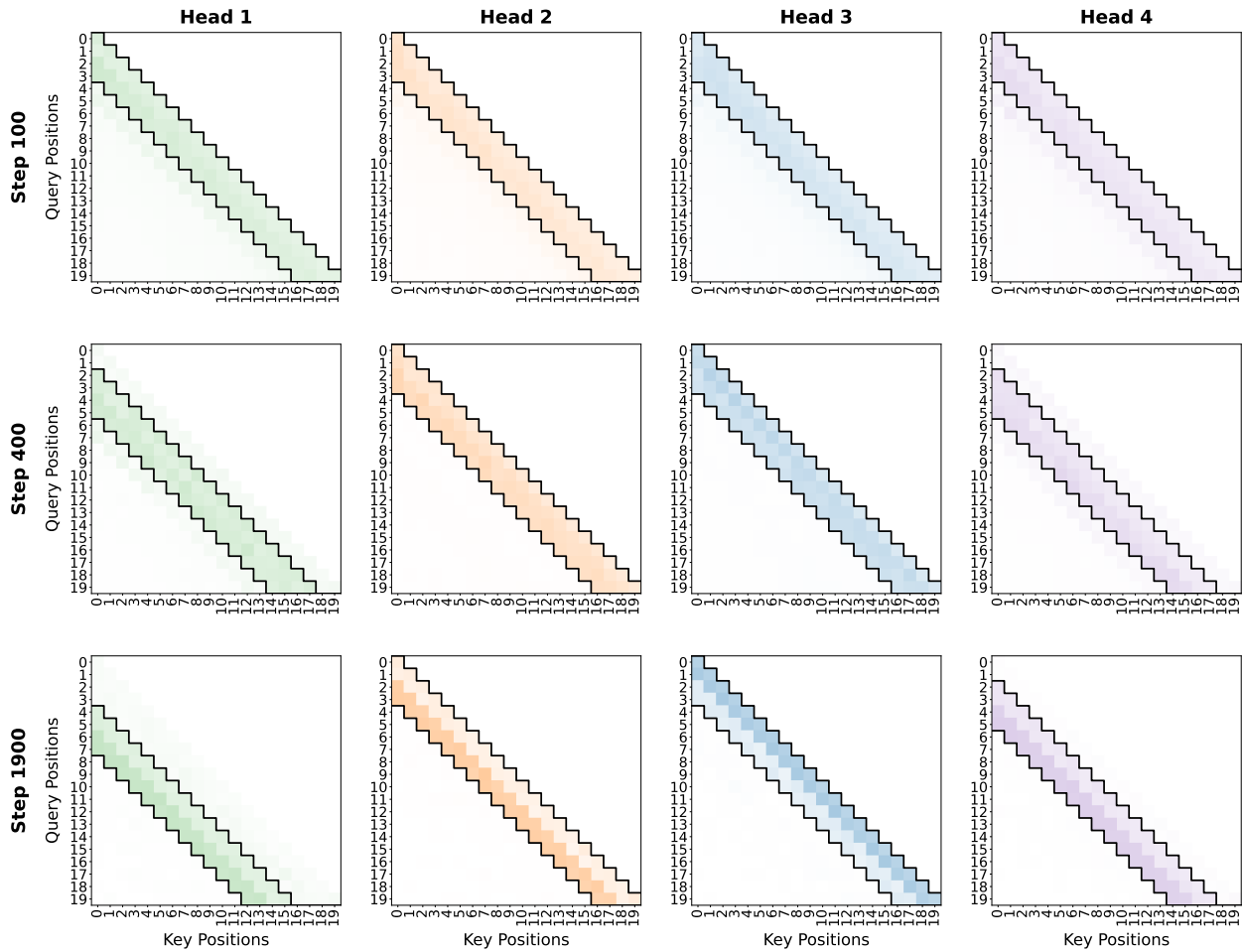


Figure 17: Attention patterns for 4 heads over the training steps with overlapping intervals.

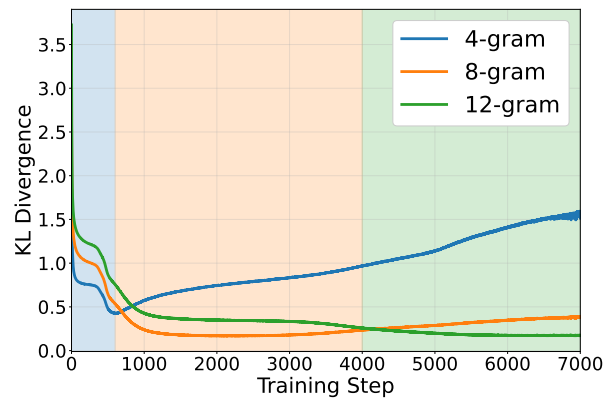


Figure 18: KL divergence over the training steps with SGD optimizer.

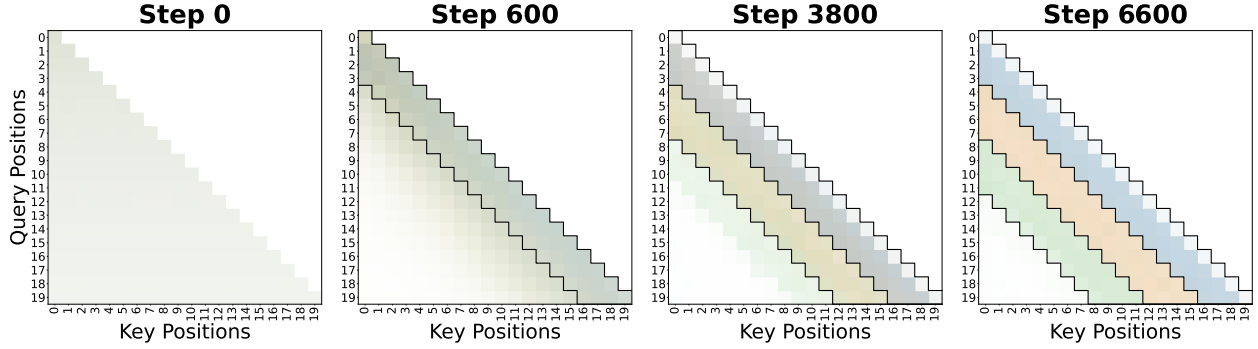


Figure 19: Attention patterns over the training steps with SGD optimizer.

Appendix C Missing Proofs

We start with the proof of Proposition 1 and some elementary results on the operation Π . Recall that we assume s_i^* are one-hot in Section 3.1. That is, in the sequel, $\|s_i^*\|^2 = 1$.

Proposition 1. *The gradient flow dynamics of the loss in Equation (4) is equivalent to that on*

$$\mathcal{L}(\theta) = \frac{1}{2} \|\mathbf{G} - \mathbf{P}\|_F^2 \quad \text{where} \quad \mathbf{P} = \sum_{k=1}^h V_k \otimes s_k, \quad \text{and} \quad \mathbf{G} = \sum_{k=1}^h m_k^* (V_k^* \otimes s_k^*).$$

Proof. We start by some computations. Note that for any vectors $v_1, v_2 \in \mathbb{R}^T$, we have:

$$\begin{aligned} \mathbb{E} \left[(Xv_1)(Xv_2)^\top \right] &= \sum_{i=1}^T \sum_{j=1}^T (v_1)_i (v_2)_j \mathbb{E} [x_i x_j^\top] \\ &= \langle v_1, v_2 \rangle I_d. \end{aligned}$$

Also, for any vectors $v_1, v_2 \in \mathbb{R}^T$ and any matrix $Q \in \mathbb{R}^{d \times d}$, we have:

$$\begin{aligned} \mathbb{E} [v_1^\top X^\top Q X v_2] &= \sum_{i=1}^T \sum_{j=1}^T (v_1)_i (v_2)_j \mathbb{E} [x_i^\top Q x_j] \\ &= \sum_{i=1}^T \sum_{j=1}^T (v_1)_i (v_2)_j \text{Tr} (Q \mathbb{E} [x_j x_i^\top]) \\ &= \langle v_1, v_2 \rangle \text{Tr}(Q). \end{aligned}$$

By selecting $v_2 = e_i$ for all $i \in [d]$, we get:

$$\mathbb{E} [v_1 X^\top Q X] = \text{Tr}(Q) v_1.$$

First, the derivative with respect to V_i is as follows:

$$\begin{aligned} \frac{\partial \mathcal{L}(\theta)}{\partial V_i} &= \mathbb{E}_{X, \xi} \left[(f_\theta(X) - f^*(X, \xi)) (X s_i)^\top \right] \\ &= \sum_{j=1}^h V_j \langle s_i, s_j \rangle - \sum_{j=1}^h m_j^* \langle s_i, s_j^* \rangle V_j^*. \end{aligned}$$

Next, the derivative with respect to q_i is as follows:

$$\begin{aligned} \frac{\partial \mathcal{L}(\theta)}{\partial q_i} &= (\text{diag}(s_i) - s_i s_i^\top) \mathbb{E}_{X, \xi} [X^\top V_i^\top (f_\theta(X) - f^*(X, \xi))] \\ &= (\text{diag}(s_i) - s_i s_i^\top) \left(\sum_{j=1}^h \langle V_i, V_j \rangle s_j - \sum_{j=1}^h m_j^* \langle V_i, V_j^* \rangle s_j^* \right). \end{aligned}$$

Then, the gradient flow dynamics is as follows:

$$\begin{aligned} \dot{V}_i &= -\nabla_{V_i} \mathcal{L}(\theta) = (\mathbf{G} - \mathbf{P}) s_i \\ \dot{q}_i &= -\nabla_{q_i} \mathcal{L}(\theta) = \Pi(s_i) (V_i^\top (\mathbf{G} - \mathbf{P})). \end{aligned}$$

This can be seen as a gradient ascent flow on the following loss:

$$\mathcal{L}(\theta) = \frac{1}{2} \|\mathbf{G} - \mathbf{P}\|_F^2.$$

□

Lemma 2. *Let s be a vector with non-negative entries and $\|s\|_1 = 1$. Then, the kernel space of $\Pi(s) = \text{diag}(s) - ss^\top$ is*

$$\ker(\Pi(s)) = \text{span}(\{e_j : \langle e_j, s \rangle = 0\}) \cup \text{span} \left(\sum_{j: \langle e_j, s \rangle > 0} e_j \right).$$

Furthermore, if $\|s\|_1 < 1$,

$$\ker(\Pi(s)) = \text{span}(\{e_j : \langle e_j, s \rangle = 0\}).$$

Proof. The proof follows trivially from a rank analysis. □

Lemma 3. *Let s be a vector on the simplex that verifies $s_i \geq s_j$ for all $j \in [h]$. Then, for any vector v that verifies $v_i \geq v_j$ for all $j \in [h]$, we have for all $j \in [h]$:*

$$(\Pi(s)v)_i \geq (\Pi(s)v)_j.$$

Proof. We have the following computations:

$$\begin{aligned} (\Pi(s)v)_i &= s_i (v_i - \langle s, v \rangle) \\ (\Pi(s)v)_j &= s_j (v_j - \langle s, v \rangle). \end{aligned}$$

Then, we have:

$$(\Pi(s)v)_i - (\Pi(s)v)_j \geq (s_i - s_j) (v_i - \langle s, v \rangle) \geq 0.$$

□

C.1 Boundedness

In this section, we prove Theorems 2 and 3 that are required to establish boundedness of the dynamics.

Theorem 2. *Assume that the following holds for $\epsilon \ll 1$:*

$$\forall k \in [h] : \|V(0) - V_k(0)\|_F \leq \epsilon \text{ and } \|s(0) - s_k(0)\|_2 \leq \epsilon.$$

Then, there exists a constant c_1 such that $\forall t \in \left[0, \frac{1}{-c_1 \log \epsilon}\right]$:

$$\|V_k(t) - V(t)\|_F \leq \epsilon e^{c_1 t} \text{ and } \|s_k(t) - s(t)\|_2 \leq \epsilon e^{c_1 t}.$$

Proof. We write the flow of V_i and s_i in terms of the flow of V and s by new variables:

$$W_i = V_i - V, \quad z_i = s_i - s.$$

Let ϵ be the following quantity:

$$\epsilon = \max_{j \in [h]} \max\{\|W_j\|_F, \|z_j\|\}.$$

We are interested in the regime where $\epsilon \ll 1$.

Recall that, $\phi(V, s)$ defined in Equation (11) is always non-decreasing. Therefore, V cannot grow larger than $\frac{\mathbf{G}s}{h\|s\|^2}$ in norm or otherwise $\phi(V, s)$ would decrease. This is the optimal value of V for a particular s . Thus,

we have a time-independent upper bound $|V| \leq \max_s \frac{\mathbf{G}s}{h\|s\|^2} = \frac{m_1^*}{h}$.

Then, the flow of W_i and z_i is as follows:

$$\begin{aligned} \dot{W}_i &= \mathbf{G}z_i - \mathbf{P}s_i + h\|s\|^2V, \\ \dot{z}_i &= \Pi(s_i)^2 (V_i^\top (\mathbf{G} - \mathbf{P})) - \Pi(s)^2 (V^\top \mathbf{G} - h\|V\|^2s). \end{aligned}$$

Note that, \mathbf{P} can be rewritten as follows:

$$\mathbf{P} = \sum_{j=1}^h V_j \otimes s_j = hV \otimes s + \left(\sum_{j=1}^h W_j \right) \otimes s + V \otimes \left(\sum_{j=1}^h z_j \right) + \left(\sum_{j=1}^h W_j \otimes z_j \right).$$

This implies that:

$$V^\top \mathbf{P} = h\|V\|^2s + \mathcal{O}(\epsilon + \epsilon^2), \quad \mathbf{P}s = h\|s\|^2V + \mathcal{O}(\epsilon + \epsilon^2).$$

We can rewrite the flow of z_i as follows:

$$\dot{z}_i = (\Pi(s_i)^2 - \Pi(s)^2) (V_i^\top (\mathbf{G} - \mathbf{P})) + \Pi(s)^2 (W_i^\top \mathbf{G} - V_i^\top \mathbf{P} + h\|V\|^2s).$$

Therefore, we have:

$$\dot{W}_i = \mathcal{O}(\epsilon), \quad \dot{z}_i = \mathcal{O}(\epsilon).$$

The norm of W_i and z_i are then evolve as follows:

$$\widehat{\|\dot{W}_i\|} = \frac{\dot{W}_i^\top W_i}{\|W_i\|} \leq \|\dot{W}_i\| = \mathcal{O}(\epsilon).$$

We similarly derive that $\|\dot{z}_i\| = \mathcal{O}(\epsilon)$.

This implies that ϵ verifies the equation:

$$\dot{\epsilon} \leq C\epsilon, \quad \text{as long as } \epsilon \ll 1,$$

where C is a constant that depends on the problem parameters h and \mathbf{G} . From the Grönwall's inequality, we have:

$$\epsilon(t) \leq \epsilon(0)e^{Ct}, \quad \text{as long as } t \in \left[0, \frac{1}{-C \log \epsilon(0)}\right].$$

□

Theorem 3. Assume that the following holds for $\epsilon \ll 1$:

$$\begin{aligned} \forall k \in [h-1]: \|V(0) - V_k(0)\|_F \leq \epsilon, \|e_1 - s_k(0)\|_2 \leq \epsilon, \\ \text{and } \|V'(0) - V_h(0)\|_F \leq \epsilon, \|s'(0) - s_h(0)\|_2 \leq \epsilon. \end{aligned}$$

Let $\Delta(t)$ be the deviation from the cooperative system in Equation (8):

$$\Delta(t) = \max \left\{ \max_k \{ \|V_k(t) - V(t)\|_F, \|s_k(t) - s(t)\|_2 \}, \right. \\ \left. \|V_h(t) - V(t)\|_F, \|s_h(t) - s(t)\|_2 \right\}.$$

Assuming that $\|s'(t) - s_1^*\| \geq \delta$ for all $t \in \mathbb{R}$, there exists a universal constant c_1 such that:

$$\Delta(t) \leq \epsilon e^{c_1 t}, \quad \forall t \in \left[0, \frac{1}{-c_1 \log \epsilon} \right].$$

Proof. We follow the same strategy as in the proof of Theorem 2. The new Lyapunov function is as follows:

$$\phi(V, V', s') = (h-1)m_1^* \langle V, V_1^* \rangle - \frac{(h-1)^2}{2} \|V\|_F^2 \\ - (h-1) \langle s_1^*, s' \rangle \langle V, V' \rangle + \langle V', \mathbf{G}s' \rangle - \frac{1}{2} \|s'\|^2 \|V'\|_F^2.$$

We have the following derivatives:

$$\nabla_V \phi(V, V', s') = (h-1)\dot{V}, \\ \nabla_{V'} \phi(V, V', s') = \dot{V}', \\ \nabla_{s'} \phi(V, V', s') = V^\top \mathbf{G} - (h-1) \langle V, V' \rangle s_1^* - \|V'\|^2 s'.$$

By a similar argument, we have that

$$\dot{\phi} = (h-1) \|\dot{V}\|^2 + \|\dot{V}'\|^2 + \|\Pi(s')\dot{s}'\|^2 \geq 0.$$

This indicates that ϕ is non-decreasing. By a similar argument to Theorem 2, we establish an upper bound to ϕ and consequentially the boundedness of the flow. Then, it is possible to show the noise process grows as $\mathcal{O}(\epsilon)$ where ϵ is the same quantity as in Theorem 2. \square

C.2 Competitive Phase

In this section, we prove the main result of Section 3.2.

Theorem 1. Assume that the initialization verifies the following for all $k \in [h]$:

$$\langle V(0), V_1^* \rangle \geq \langle V(0), V_k^* \rangle, \quad \langle s(0), s_1^* \rangle \geq \langle s(0), s_k^* \rangle. \quad (5)$$

Then, the dynamics of V and s converge to the following fixed point:

$$V(\infty) = \frac{m_1^*}{h} V_1^*, \quad s(\infty) = s_1^*. \quad (6)$$

Proof. Let \mathcal{R} be the following set:

$$\mathcal{R} = \{ (V, s) \mid \forall k \in [h], \langle V, V_1^* - V_k^* \rangle \geq 0, \langle s, s_1^* - s_k^* \rangle \geq 0 \}.$$

We prove that the flow is forward-invariant on \mathcal{R} .

Fix any $j \in [h]$. Let $w_j = \langle V, V_1^* - V_j^* \rangle$, $z_j = \langle s, s_1^* - s_j^* \rangle$, $r_j = \langle s \odot s, s_1^* - s_j^* \rangle$, $t_j = \langle s \odot s \odot s, s_1^* - s_j^* \rangle$. The flow of w_j and z_j are as follows:

$$\dot{w}_j = m_1^* \langle s, s_1^* \rangle - m_j^* \langle s, s_j^* \rangle - h \|s\|^2 w_j, \\ \dot{z}_j = (s_1^* - s_j^*)^\top \Pi(s)^2 (V^\top \mathbf{G} - h \|V\|_F^2 s).$$

Rewriting the derivative of \dot{z}_j :

$$\begin{aligned}
\dot{z}_j &= ((s_1^* - s_j^*)^\top \text{diag}(s) - z_j s^\top) \Pi(s) (V^\top \mathbf{G} - h \|V\|_F^2 s) \\
&= (s_1^* - s_j^*)^\top \text{diag}(s)^2 (V^\top \mathbf{G} - h \|V\|_F^2 s) - z_j s^\top \text{diag}(s) (V^\top \mathbf{G} - h \|V\|_F^2 s) \\
&\quad + (\|s\|^2 z_j - r_j) (V^\top \mathbf{G} s - h \|V\|_F^2 \|s\|^2) \\
&= m_1^* \langle s_1^*, s \rangle^2 \|s_1^*\|^2 \langle V, V_1^* \rangle - m_j^* \langle s_j^*, s \rangle^2 \|s_j^*\|^2 \langle V, V_j^* \rangle - h \|V\|_F^2 t_j \\
&\quad - z_j s^\top \text{diag}(s) (V^\top \mathbf{G} - h \|V\|_F^2 s) + (\|s\|^2 z_j - r_j) (V^\top \mathbf{G} s - h \|V\|_F^2 \|s\|^2).
\end{aligned}$$

On the boundary of \mathcal{R} , we have $w_j = 0$ or $z_j = 0$. If $w_j = 0$, then $\dot{w}_j \geq 0$ and if $z_j = 0$, then $r_j = t_j = 0$ and $\dot{z}_j \geq 0$. Therefore, a flow that has started in \mathcal{R} will remain in \mathcal{R} for all time.

Now, consider the following Lyapunov function:

$$\phi(V, s) = \langle V, \mathbf{G}s \rangle - \frac{h}{2} \|V\|_F^2 \|s\|^2. \quad (11)$$

The derivative of $\phi(V, s)$ is as follows:

$$\begin{aligned}
\nabla_V \phi(V, s) &= \mathbf{G}s - h \|s\|^2 V, \\
\nabla_s \phi(V, s) &= V^\top \mathbf{G} - h \|V\|_F^2 s.
\end{aligned}$$

Therefore, the time derivative of ϕ :

$$\dot{\phi}(V, s) = \|\dot{V}\|^2 + \|\Pi(s) \nabla_s \phi(V, s)\|^2 \geq 0.$$

ϕ is optimized when $V = \frac{\mathbf{G}s}{h \|s\|^2}$ which leads to a finite value upper bound on $\phi(V, s)$. Therefore, $\lim_{t \rightarrow \infty} \phi(V(t), s(t))$ is finite and the flow converges to a stationary point of ϕ . That is, the flow converges to a point (V_∞, s_∞) that verifies:

$$\mathbf{G}s_\infty - h \|s_\infty\|^2 V_\infty = 0, \quad V_\infty^\top \mathbf{G} - h \|V_\infty\|_F^2 s_\infty \in \ker(\Pi(s_\infty)).$$

Note that, we have the following equality:

$$(\mathbf{G}s_\infty)^\top \mathbf{G} = \sum_{j=1}^h m_j^* \left\langle V_j^*, \sum_{k=1}^h m_k^* V_k^* \langle s_k^*, s_\infty \rangle \right\rangle s_j^* = \sum_{j=1}^h (m_j^*)^2 \langle s_j^*, s_\infty \rangle s_j^*.$$

Then, the stationary point (V_∞, s_∞) verifies

$$\sum_{j=1}^h (m_j^*)^2 \langle s_j^*, s_\infty \rangle s_j^* - h^2 \|s_\infty\|^2 \|V_\infty\|_F^2 \langle s_1^*, s_\infty \rangle s_1^* \in \ker(\Pi(s_\infty)). \quad (12)$$

We have proven that $\langle s_1^*, s_\infty \rangle > 0$ as $\langle s_1^*, s_\infty \rangle = \max_{k \in [h]} \langle s_k^*, s_\infty \rangle$. From Lemma 2, $s_1^* \notin \ker(\Pi(s_\infty))$ as there is at least one index $m \in [T]$ such that $\langle e_m, s_\infty \rangle > 0$ and $\langle e_m, s_1^* \rangle > 0$. By projecting to the direction s_1^* , Equation (12) implies

$$(m_1^*)^2 \langle s_1^*, s_\infty \rangle - h^2 \|s_\infty\|^2 \|V_\infty\|_F^2 \langle s_1^*, s_\infty \rangle = 0.$$

However, note that

$$h^2 \|s_\infty\|^2 \|V_\infty\|_F^2 = \frac{\|\mathbf{G}s_\infty\|^2}{\|s_\infty\|^2} \leq \max_{\|s\|=1} \|\mathbf{G}s\|^2 = (m_1^*)^2,$$

with equality if and only if $s_\infty = s_1^*$. Therefore, the flow converges to the stationary point

$$s = s_1^*, \quad V = \frac{m_1^*}{h} V_1^*.$$

□

C.3 Cooperation Phase

In this section, we prove the remaining results in Section 3.3. First, we show convergence of the second head starting with the system in Equation (8). Later, we extend the analysis to any arbitrary phase in the dynamics.

C.3.1 Convergence of the Second Head

Following Equation (7), we consider the following initialization scheme:

$$V(0) = \frac{1}{h-1} (m_1^* V_1^* - \langle s_1^*, s'(0) \rangle V'(0)), \quad V'(0) \approx V(0), \quad s'(0) \approx s_1^*. \quad (13)$$

Here, we note that $\dot{V}(0) = 0$. That is, $V(0)$ is at its optimal value given $V'(0)$ and $s'(0)$. The following lemma shows that V stays close to its optimum through the trajectory:

Lemma 1. *Let $\Delta(t) = V(t) - V^*(t)$ where*

$$V^*(t) = \frac{1}{h-1} (m_1^* V_1^* - \langle s_1^*, s'(t) \rangle V'(t)).$$

Assuming that $\|s'(t) - s_1^\| \geq \delta$ for all $t \in \mathbb{R}$, there exist constants $c_1(\delta), c_2$ such that*

$$\|\Delta(t)\|_F \leq e^{-c_2 t} \|\Delta(0)\|_F + \frac{c_1(\delta)}{c_2}.$$

Proof. Let's compute the derivative of Δ :

$$\dot{\Delta} = -(h-1)\|s_1^*\|^2 \Delta + \frac{1}{h-1} \langle s_1^*, s' \rangle \dot{V}' + \frac{1}{h-1} \langle s_1^*, \dot{s}' \rangle V'.$$

Then, setting $c_2 = \frac{(h-1)}{2} \|s_1^*\|^2$ and $c(t) = \frac{1}{h-1} \langle s_1^*, s'(t) \rangle V'(t)$

$$\widehat{\|\Delta(t)\|_F^2} = 2\langle \dot{\Delta}(t), \Delta(t) \rangle = -2c_2 \|\Delta(t)\|_F^2 + 2\langle \dot{c}(t), \Delta(t) \rangle.$$

We bound the last term as follows:

$$\langle \dot{c}(t), \Delta(t) \rangle \leq \|\dot{c}(t)\|_F \|\Delta(t)\|_F.$$

However, $\dot{c}(t)_F$ is uniformly bounded as in Theorem 3, so we get:

$$\widehat{\|\Delta(t)\|_F^2} \leq -2c_2 \|\Delta(t)\|_F^2 + 2c_1 \|\Delta(t)\|_F.$$

Set $u(t) = \|\Delta(t)\|_F - \frac{c_1}{c_2}$ and rewrite the inequality:

$$\dot{u}(t) \leq -c_2 u(t).$$

By Grönwall's inequality, we have the desired result. \square

Based on Lemma 1 and evidence from our numerical simulations, we approximate the full dynamics by a two-scale analysis where V is optimized faster than V' and s' , leading to Equation (9). Expanding $\Pi(s')$, we get

$$\Pi(s') = \Pi(s'_{(1)}) + \langle s_1^*, s' \rangle \left(s_1^* (s_1^*)^\top - s_1^* s'_{(1)}^\top - s'_{(1)} (s_1^*)^\top \right).$$

Since, the $V'_{(1)}^\top \mathbf{G}_{(1)} - \|V'\|_F^2 s'_{(1)}$ is perpendicular to the direction s_1^* , we obtain:

$$\dot{s}' = \Pi(s') \left(\Pi(s'_{(1)}) - \langle s_1^*, s' \rangle s_1^* s'_{(1)}^\top \right) \left(V'_{(1)}^\top \mathbf{G}_{(1)} - \|V'\|_F^2 s'_{(1)} \right).$$

Writing out the update along the direction of s_1^* :

$$\begin{aligned}\langle s_1^*, \dot{s}' \rangle &= \langle s_1^*, s' \rangle \|s_1^*\|^2 \left(s_1^* - s'_{(1)} \right)^\top \left(\Pi(s'_{(1)}) - \langle s_1^*, s' \rangle s_1^* s'_{(1)}^\top \right) \left(V'_{(1)}{}^\top \mathbf{G}_{(1)} - \|V'\|_F^2 s'_{(1)} \right) \\ &= -\langle s_1^*, s' \rangle \|s_1^*\|^2 s'_{(1)}^\top \left(\Pi(s'_{(1)}) + \langle s_1^*, s' \rangle \|s_1^*\|^2 I \right) \left(V'_{(1)}{}^\top \mathbf{G}_{(1)} - \|V'\|_F^2 s'_{(1)} \right).\end{aligned}$$

The rest of the update follows:

$$\begin{aligned}\dot{s}'_{(1)} &= \left(\Pi(s'_{(1)}) - \langle s_1^*, s' \rangle s'_{(1)} (s_1^*)^\top \right) \left(\Pi(s'_{(1)}) - \langle s_1^*, s' \rangle s_1^* s'_{(1)}^\top \right) \left(V'_{(1)}{}^\top \mathbf{G}_{(1)} - \|V'\|_F^2 s'_{(1)} \right) \\ &= \left(\Pi(s'_{(1)})^2 + \langle s_1^*, s' \rangle^2 \|s_1^*\|^2 s'_{(1)} s'_{(1)}^\top \right) \left(V'_{(1)}{}^\top \mathbf{G}_{(1)} - \|V'\|_F^2 s'_{(1)} \right).\end{aligned}$$

Similarly, writing the update for $V'_{(1)}$ and the update in the direction of V_1^* :

$$\begin{aligned}\langle V_1^*, \dot{V}' \rangle &= -\|s'_{(1)}\|^2 \langle V_1^*, \dot{V}' \rangle, \\ \dot{V}'_{(1)} &= \mathbf{G}_{(1)} s'_{(1)} - \|s'_{(1)}\|^2 V'_{(1)}.\end{aligned}$$

We are ready to state the main theorem:

Theorem 4. *Assume that the initialization verifies the following for all $k \in [2, h]$:*

$$\langle V'(0), V_2^* \rangle \geq \langle V'(0), V_k^* \rangle \quad \langle s'(0), s_2^* \rangle \geq \langle s'(0), s_k^* \rangle.$$

Further, suppose that $V'(0), s'(0)$ are such that

$$\langle V'_{(1)}(0), \mathbf{G}_{(1)} s'_{(1)}(0) \rangle > \frac{1}{2} \|V'(0)\|_F^2 \|s'_{(1)}(0)\|^2. \quad (10)$$

Then, the dynamics of V' and s' converge to the following fixed point:

$$V'(\infty) = V_2^*, \quad s'(\infty) = s_2^*.$$

Proof. We follow the same strategy as in Theorem 1. Let \mathcal{R} be the following set:

$$\mathcal{R} = \{ (V', s') \mid \forall k \in [2, h], \langle V', V_2^* \rangle \geq \langle V', V_k^* \rangle \text{ and } \langle s', s_2^* \rangle \geq \langle s', s_k^* \rangle \}.$$

We prove that the flow is forward-invariant on \mathcal{R} .

Fix any $j \in [2, h]$. Let $w_j = \langle V', V_2^* - V_j^* \rangle$ and $z_j = \langle s'_{(1)}, s_2^* - s_j^* \rangle$. The flow of w_j and z_j are as follows:

$$\begin{aligned}\dot{w}_j &= m_2^* \langle s'_{(1)}, s_2^* \rangle - m_j^* \langle s'_{(1)}, s_j^* \rangle - \|s'_{(1)}\|^2 w_j, \\ \dot{z}_j &= (s_2^* - s_j^*)^\top \left(\Pi(s'_{(1)})^2 + \langle s_1^*, s' \rangle^2 \|s_1^*\|^2 s'_{(1)} s'_{(1)}^\top \right) \left(V'_{(1)}{}^\top \mathbf{G}_{(1)} - \|V'\|_F^2 s'_{(1)} \right).\end{aligned}$$

Rewriting the derivative of \dot{z}_j :

$$\begin{aligned}\dot{z}_j &= (s_2^* - s_j^*)^\top \Pi(s'_{(1)})^2 \left(V'_{(1)}{}^\top \mathbf{G}_{(1)} - \|V'\|_F^2 s'_{(1)} \right) + cz_j \\ &= (s_2^* - s_j^*)^\top \text{diag}(s'_{(1)})^2 \left(V'_{(1)}{}^\top \mathbf{G}_{(1)} - \|V'\|_F^2 s'_{(1)} \right) \\ &\quad - (s_2^* - s_j^*)^\top \text{diag}(s'_{(1)}) s'_{(1)} s'_{(1)}^\top \left(V'_{(1)}{}^\top \mathbf{G}_{(1)} - \|V'\|_F^2 s'_{(1)} \right) + cz_j \\ &= (s_2^* - s_j^*)^\top \text{diag}(s'_{(1)})^2 \left(V'_{(1)}{}^\top \mathbf{G}_{(1)} - \|V'\|_F^2 s'_{(1)} \right) \\ &\quad - \left(\langle s'_{(1)}, s_2^* - s_j^* \rangle s_2^* + \langle s'_{(1)}, s_j^* \rangle (s_2^* - s_j^*) \right)^\top s'_{(1)} s'_{(1)}^\top \left(V'_{(1)}{}^\top \mathbf{G}_{(1)} - \|V'\|_F^2 s'_{(1)} \right) + cz_j \\ &= m_2^* \langle s_2^*, s'_{(1)} \rangle^2 \|s_2^*\|^2 \langle V', V_2^* \rangle - m_j^* \langle s_j^*, s'_{(1)} \rangle^2 \|s_j^*\|^2 \langle V', V_j^* \rangle + cz_j,\end{aligned}$$

where c is some arbitrary time-dependent function that changes from line to line. On the boundary of \mathcal{R} , we have $w_j = 0$ or $z_j = 0$. If $w_j = 0$, then $\dot{w}_j \geq 0$ and if $z_j = 0$, then $\dot{z}_j \geq 0$. Therefore, a flow that has started in \mathcal{R} will remain in \mathcal{R} for all time.

Now, consider the following Lyapunov function:

$$\phi(V', s'_{(1)}) = \langle V', \mathbf{G}_{(1)} s'_{(1)} \rangle - \frac{1}{2} \|V'\|_F^2 \|s'_{(1)}\|^2.$$

The derivative of $\phi(V', s'_{(1)})$ is as follows:

$$\begin{aligned} \nabla_{V'} \phi(V', s'_{(1)}) &= \mathbf{G}_{(1)} s'_{(1)} - \|s'_{(1)}\|^2 V', \\ \nabla_{s'_{(1)}} \phi(V', s'_{(1)}) &= V'^{\top} \mathbf{G}_{(1)} - \|V'\|_F^2 s'_{(1)}. \end{aligned}$$

Therefore, the time derivative of ϕ :

$$\dot{\phi} = \|\dot{V}'\|^2 + \|\tilde{\Pi}(s') \nabla_{s'_{(1)}} \phi(V', s')\|^2 \geq 0,$$

where $\tilde{\Pi}(s')$ is a positive semi-definite matrix that verifies:

$$\tilde{\Pi}(s')^2 = \left(\Pi(s'_{(1)})^2 + \langle s_1^*, s' \rangle^2 \|s_1^*\|^2 s'_{(1)} s'_{(1)}^{\top} \right), \quad \ker(\tilde{\Pi}(s')) \subseteq \ker(\Pi(s'_{(1)})).$$

By Equation (10),

$$\phi(0) = \phi(V'(0), s'_{(1)}(0)) > 0,$$

and $s'_{(1)} \neq 0$ as ϕ is increasing. ϕ is optimized when $V' = \frac{\mathbf{G}_{(1)} s'_{(1)}}{\|s'_{(1)}\|^2}$ which leads to a finite value upper bound on $\phi(V', s'_{(1)})$. Therefore, $\lim_{t \rightarrow \infty} \phi(V'(t), s'_{(1)}(t))$ is finite and the flow converges to a stationary point of ϕ . That is, the flow converges to a point $(V'_{\infty}, s'_{\infty})$ that verifies:

$$\mathbf{G}_{(1)} s'_{\infty} - \|s'_{\infty}\|^2 V'_{\infty} = 0, \quad V'_{\infty}^{\top} \mathbf{G}_{(1)} - \|V'_{\infty}\|_F^2 s'_{\infty} \in \ker(\Pi(s'_{\infty})).$$

Note that, we have the following equality:

$$(\mathbf{G}_{(1)} s_{\infty})^{\top} \mathbf{G}_{(1)} = \sum_{j=2}^h m_j^* \left\langle V_j^*, \sum_{k=2}^h m_k^* V_k^* \langle s_k^*, s'_{\infty} \rangle \right\rangle s_j^* = \sum_{j=2}^h (m_j^*)^2 \langle s_j^*, s'_{\infty} \rangle s_j^*.$$

Then, the stationary point $(V'_{\infty}, s'_{\infty})$ verifies

$$\sum_{j=2}^h (m_j^*)^2 \langle s_j^*, s'_{\infty} \rangle s_j^* - h^2 \|s'_{\infty}\|^2 \|V'_{\infty}\|_F^2 \langle s_j^*, s'_{\infty} \rangle s_j^* \in \ker(\Pi(s'_{\infty})).$$

We have proven that $\langle s_2^*, s'_{\infty} \rangle > 0$ as $\langle s_2^*, s'_{\infty} \rangle = \max_{k \in [2, h]} \langle s_k^*, s'_{\infty} \rangle$. From Lemma 2, $s_2^* \notin \ker(\Pi(s'_{\infty}))$. By projecting to the direction s_2^* ,

$$(m_2^*)^2 \langle s_2^*, s'_{\infty} \rangle - h^2 \|s'_{\infty}\|^2 \|V'_{\infty}\|_F^2 \langle s_2^*, s'_{\infty} \rangle = 0.$$

However, note that

$$h^2 \|s'_{\infty}\|^2 \|V'_{\infty}\|_F^2 = \frac{\|\mathbf{G}_{(1)} s'_{\infty}\|^2}{\|s'_{\infty}\|^2} \leq \max_{\|s\|=1} \|\mathbf{G}_{(1)} s\|^2 = (m_2^*)^2,$$

with equality if and only if $s_{\infty} = s_2^*$. Therefore, the flow converges to the stationary point

$$s = s_2^*, \quad V = m_2^* V_2^*.$$

□

Lastly, we justify the initialization assumption in Equation (10). Theorems 1 and 2 demonstrate that a wide range of symmetric initializations converge toward the configuration defined in Equation (13). Note that Equation (10) requires stronger alignment than Equation (13), specifically that the tensor factorization loss is strictly lower than the value attained at the first saddle point characterized by Theorem 4. In practice, this condition is satisfied by a small perturbation along the second positional feature:

Remark 2. Equation (10) is satisfied by the following initialization

$$V'(0) \approx \frac{m_1^*}{h} V_1^* + \epsilon V_2^*, \quad s'(0) \approx (1 - \epsilon) s_1^* + \epsilon s_2^*,$$

for small $\epsilon > 0$.

C.4 Extension to Higher-order Heads

Similar to Section C.3, we study the offshoot of an arbitrary head $n > 2$ after the system has learned the first $n - 1$ features. The features $2, 3, \dots, n - 1$ are all learned by a single head whereas the ensemble of $h - n$ heads are still on the first feature. This leads to the following dynamics similar to Equation (8):

$$V_1 = V_{n+1} = \dots = V_h = V, \quad s_1 = s_{n+1} = \dots = s_h = s_1^*, \quad s_2 = s_2^*, \dots, s_{n-1} = s_{n-1}^*.$$

We assume an analog of the initialization in Equation (13):

$$\begin{aligned} V(0) &= \frac{1}{h - n + 1} (m_1^* V_1^* - \langle s_1^*, s_n \rangle V_n(0)), \\ V_i(0) &= m_i^* V_i^* - \langle s_i^*, s_n \rangle V_n(0), \quad \forall i \in [2, n - 1], \\ V_n(0) &\approx V(0), \quad s_n(0) \approx s_1^*. \end{aligned}$$

This leads to a similar dynamics after assuming V, V_2, \dots, V_{n-1} has fast dynamics by a similar argument to Lemma 1 where we write $V' = V_n$ and $s' = s_n$ for brevity:

$$\begin{aligned} \dot{V}' &= \mathbf{G}_{(n-1)}(s_n)_{(n-1)} - \|(s_n)_{(n-1)}\|^2 V_n, \\ \dot{s}' &= \Pi(s_n)^2 \left(V_n^\top \mathbf{G}_{(n-1)} - \|V_n\|_F^2 (s_n)_{(n-1)} \right). \end{aligned}$$

Computing the update for in the relevant directions of s' :

$$\dot{s}'_{(n-1)} = \left(\Pi(s'_{(n-1)})^2 + \sum_{j=1}^{n-1} \langle s_j^*, s' \rangle^2 \|s_j^*\|^2 s'_{(n-1)} s'_{(n-1)}^\top \right) \left(V'^\top \mathbf{G}_{(n-1)} - \|V'\|_F^2 s'_{(n-1)} \right).$$

The same analysis in Section C.3.1 leads to the following theorem:

Theorem 5. Assume that the initialization verifies the following for all $k \in [n, h]$:

$$\langle V_n(0), V_n^* \rangle \geq \langle V_n(0), V_k^* \rangle \quad \langle s_n(0), s_n^* \rangle \geq \langle s_n(0), s_k^* \rangle.$$

Further, suppose that $V_n(0), s_n(0)$ are such that

$$\langle V_n(0), \mathbf{G}_{(n-1)}(s_n)_{(n-1)}(0) \rangle > \frac{1}{2} \|V_n(0)\|_F^2 \|(s_n)_{(n-1)}\|^2.$$

Then, the dynamics of V_n and s_n converge to the following fixed point:

$$V_n(\infty) = V_n^*, \quad s_n(\infty) = s_n^*.$$

Proof. The proof proceeds mutatis mutandis to that of Theorem 4. □

Appendix D Expanding the Initialization Condition

In this section, we explain Remark 1 in detail. As stated, for any initialization around $s_k(0) \approx \frac{1}{T} \mathbf{1}_T$ and $V_k \approx 0$, we obtain the following from the first-order Taylor approximation as $\mathbf{P} \approx 0$:

$$\dot{V}_k(0) \approx \frac{1}{T} \mathbf{G} \mathbf{1}_T, \quad \dot{s}_k(0) \approx 0.$$

Therefore, the heads $V_k(0)$ exhibit a faster dynamics than the attention scores s_k . For small timescales t , the heads are approximately aligned with the same direction:

$$V_k(t) \approx \frac{t}{T} \mathbf{G} \mathbf{1}_T,$$

which satisfies the initialization condition in Theorem 1 as $m_1^* \geq m_k^*$ for any $k \in [h]$. Moreover, the second-order Taylor approximation yields:

$$\begin{aligned} \ddot{V}_k(0) &\approx - \sum_i \dot{V}_i s_i^\top s_k \approx \frac{1}{T^2} \mathbf{G} \mathbf{1}_T, \\ \ddot{s}_k(0) &\approx \Pi(s_k) \dot{V}_k^\top (\mathbf{G} - \mathbf{P}) \approx \frac{1}{T} \pi(s_k) \mathbf{G} \mathbf{1}_T. \end{aligned}$$

By, Lemma 3, we can show that $\dot{s}_k(0)$ is such that the component of s_1^* is the maximal entry. Therefore, we expect s_k to align towards the initialization condition given in Theorem 1 for small timescales t :

$$s_k(t) \approx \frac{1}{T^2} \left(I_T - \frac{1}{T} \mathbf{1}_T \mathbf{1}_T^\top \right) \mathbf{G} \mathbf{1}_T.$$

Similar type of analysis also applies to the initializations of Theorems 4 and 5.

Note that the initialization regimes in our theorems are not towards a particular point but a large set that verifies some ordering. Coupled with the analysis above, the initialization basin for these theorems can be expanded. This contrasts with analyses that rely on vanishing initialization or limits towards critical submanifolds.